

AD 678493

AD

USAAVLABS TECHNICAL REPORT 68-48

DESIGN AND COMPONENT TEST OF ENGINE AIR INLET PARTICLE SEPARATOR FOR THE CV-7A AIRCRAFT

By

R. J. Duffy

August 1968

U. S. ARMY AVIATION MATERIEL LABORATORIES
FORT EUSTIS, VIRGINIA

CONTRACT DA 44-177-AMC-343(T)
GENERAL ELECTRIC COMPANY
WEST LYNN, MASSACHUSETTS

*This document has been approved
for public release and sale; its
distribution is unlimited.*



CLASSIFIED

79

Disclaimers

The findings in this report are not to be construed as an official Department of the Army position unless so designated by other authorized documents.

When Government drawings, specifications, or other data are used for any purpose other than in connection with a definitely related Government procurement operation, the United States Government thereby incurs no responsibility nor any obligation whatsoever; and the fact that the Government may have formulated, furnished, or in any way supplied the said drawings, specifications, or other data is not to be regarded by implication or otherwise as in any manner licensing the holder or any other person or corporation, or conveying any rights or permission, to manufacture, use, or sell any patented invention that may in any way be related thereto.

Disposition Instructions

Destroy this report when no longer needed. Do not return it to originator.

STH		RECEIVED
EDC	BUFF SECTION <input type="checkbox"/>	
UNCLASSIFIED	<input type="checkbox"/>	
JUSTIFICATION		
.....		
-Y		
DISTRIBUTION/AVAILABILITY CODES		
DIST.	AVAIL.	and/or SPECIAL
1		



DEPARTMENT OF THE ARMY
U. S. ARMY AVIATION MATERIEL LABORATORIES
FORT EUSTIS, VIRGINIA 23604

This report was prepared by the General Electric Company under the terms of Contract DA 44-177-AMT-343(T). The contractual action was undertaken at the request of the CV-7A Project Manager.

The original intent of the effort was to design, fabricate, and laboratory test an engine inlet air particle separator for the CV-7A and to deliver to the Army one set of flight hardware for installation on a CV-7A. During the course of this effort, the CV-7A was assigned to the U.S. Air Force. Subsequently, the Army program was discontinued upon completion of bench testing.

The conclusions and recommendations contained herein are generally concurred in by this command.

Project 1T062103A047
Contract DA 44-177-AMC-343(T)
USAAVLABS Technical Report 68-48
August 1968

DESIGN AND COMPONENT TEST OF ENGINE AIR
INLET PARTICLE SEPARATOR FOR THE CV-7A AIRCRAFT

Final Report

By
R. J. Duffy

Prepared by
General Electric Company
West Lynn, Massachusetts

For
U. S. ARMY AVIATION MATERIEL LABORATORIES
FORT EUSTIS, VIRGINIA

This document has been approved
for public release and sale; its
distribution is unlimited.

SUMMARY

An inlet protection system for the CV-7A aircraft's T64-GE-8 engine is described in this report. Separator design, special manufacturing problems, and component test results are presented and discussed. Additional background information describing previous work from which the CV-7A separator design evolved is included where applicable.

Component efficiency tests indicate that separator collection efficiencies exceed contract requirements. Pressure loss measurements, taken coincident with the efficiency tests, indicate a pressure drop greater than design limits. Engine testing, not included in the modified contract work scope, would be required to accurately define the result of increased pressure loss on installed engine performance.

FOREWORD

The original scope of the work requested by Contract DA 44-177-AMC-343(T) was to design, factory test, and flight test an inlet protection device for one engine of the twin-engine CV-7A aircraft. Modification No. 1 to the contract limited the work scope to bench testing the separators. Consequently, only two separators (sufficient for one T64-GE-8 engine) were manufactured. All other hardware required for the complete inlet protection system was shipped in the "in process" condition.

Original development design work on which the CV-7A separator design was based was done under Contract AF33(657)1244.

TABLE OF CONTENTS

	<u>Page</u>
SUMMARY	iii
FOREWORD	v
LIST OF ILLUSTRATIONS	viii
LIST OF TABLES	xi
LIST OF SYMBOLS	xii
INTRODUCTION	1
DESCRIPTION OF TEST ARTICLE	4
Basic Separator	4
CV-7A Design	4
SEPARATOR INSTALLATION	8
TEST SETUP AND EXPERIMENTAL PROCEDURE	11
TEST RESULTS	15
DISCUSSION OF TEST DATA	19
Collection Efficiency Results	19
Extrapolation of Data to Higher Flows	19
Testing with AC Coarse Dust	22
PRESSURE LOSS TESTS	25
DESIGN IMPROVEMENTS	26
CONCLUSIONS	28
RECOMMENDATIONS	29
LITERATURE CITED	30
APPENDIXES	
I - PRESSURE PROFILES	32
II - PRELIMINARY EVALUATION OF DUST-SEPARATOR	40
III - TEST RESULTS OF SEPARATOR DESIGN IMPROVEMENTS ON FULL-SCALE FLOW MODEL	57
DISTRIBUTION	66

LIST OF ILLUSTRATIONS

<u>Figure</u>		<u>Page</u>
1	Test Setup of CV-7A Duct Model and Serial Number 2 Separator	2
2	Test Setup Showing Axial Scroll and Scavenge Discharge .	3
3	Inlet Separator	4
4	CV-7A Separator Cross Section	5
5	Particle Separator Axial Scroll	6
6	Installation of Twin Separators	9
7	Pressure Drop Rake	12
8	Separator Test Facility Airflow Calibration Curve	13
9	Pressure Loss Across Separator	16
10	Pressure Loss Across Separator	16
11	CV-7A Separator Collection Efficiency vs Particle Size ..	17
12	CV-7A Separator Collection Efficiency vs Particle Size ..	17
13	Radial Total Pressure Profile	18
14	738 Design Test Efficiency on 0 to 1000 Micron Sand	20
15	Efficiency of the General Electric Model No. 9899537-738 Inlet Particle Separator as a Function of Engine Airflow .	21
16	Test Dust Distributions Showing Cutoff Size	22
17	Particle Separator Efficiency With Scavenge	23
18	Inlet Separator - Exit Guide Vane Losses vs Radius Ratio.	26
19	Wake Rake Span Across Exit Vane Spacings	32
20	Wake Rake Readings - Immersion 6	33
21	Wake Rake Readings - Immersion 5	34
22	Wake Rake Readings - Immersion 4	35
23	Wake Rake Readings - Immersion 3	36

<u>Figure</u>		<u>Page</u>
24	Wake Rake Readings - Immersion 2	37
25	Wake Rake Readings - Immersion 1	38
26	Wake Rake Traverse by Two Different Integration Procedures	39
27	CV-7A/T64 Inlet Duct - Pressure Recovery for Basic Duct and Separator Installation Configuration	42
28	CV-7A/T64 Inlet Duct - Circumferential Distortion Average Across Annulus	42
29	CV-7A/T64 Inlet Duct - Distortion Pattern at Flow of 7.97 Lb/Sec With Separator	44
30	CV-7A/T64 Inlet Duct - Distortion Pattern at Flow of 8.78 Lb/Sec With Separator	44
31	CV-7A/T64 Inlet Duct - Distortion Pattern at Flow of 9.3 Lb/Sec With Separator	45
32	CV-7A/T64 Inlet Duct - Distortion Pattern at Flow of 9.4 Lb/Sec With Separator	45
33	CV-7A/T64 Inlet Duct - Distortion Pattern at Flow of 10.1 Lb/Sec With Separator	46
34	CV-7A/T64 Inlet Duct - Distortion Pattern at Flow of 8.11 Lb/Sec Without Separator	46
35	CV-7A/T64 Inlet Duct - Distortion Pattern at Flow of 9.12 Lb/Sec Without Separator	47
36	CV-7A/T64 Inlet Duct - Distortion Pattern at Flow of 11.7 Lb/Sec Without Separator	47
37	CV-7A/T64 Inlet Duct - Average Radial Distortion With Separator	48
38	CV-7A/T64 Inlet Duct - Radial Distortion at $92.5\% N_G / \sqrt{\theta_2}$ With Separator	48
39	CV-7A/T64 Inlet Duct - Average and Maximum Angular Radial Distortion	49

<u>Figure</u>		<u>Page</u>
40	CV-7A/T64 Inlet Duct - Static Pressures Along Duct Flow - 11.7 Lb/Sec Without Separator	50
41	CV-7A/T64 Inlet Duct - Static Pressures Along Duct Flow - 10.1 Lb/Sec With Separator	50
42	CV-7A/T64 Inlet Duct - Static Probe Locations	51
43	CV-7A/T64 Test Duct and Separator Layout	51
44	CV-7A/T64 Inlet Duct - Schematic of Test Duct Looking Downstream Showing Rake and Test Positions	52
45	Full-Scale Flow Model on Component Test Stand	58
46	Comparison of Lip Shapes	58
47	Schematic Cross Section of Separator Flow Model Showing Various Modifications	59
48	Number 1 Hub Hump on Separator Aft Wall	59
49	Total Pressure Profiles Aft of Separator	63
50	Schematic Cross Section of Separator Flow Model, Showing Most Promising Changes	65

LIST OF TABLES

<u>Table</u>		<u>Page</u>
I	Test Sands	14
II	Collection Efficiency on AC Coarse Dust	15
III	Separation Efficiencies	20
IV	Radial Distortion	55
V	Pressure Recovery and Horsepower Loss at 25 Lb/Sec Flow	56
VI	Test Summary	62

LIST OF SYMBOLS

η_c	collection efficiency, percent
PPS	pounds per second, lb/sec
η_{c1}	efficiency of T58 design at 11 PPS, percent
η_{c2}	efficiency of T58 design at 12.5 PPS, percent
\approx	approximate value
P2 Max	highest total pressure in the sectors under consideration at a given diameter
P2 Min	lowest total pressure in the sector under consideration at the same diameter as P2 Max
P2 Ave	area weighted average total pressure at the same diameter as P2 Max
Θ_1^-	single low-pressure area in compressor annulus, measured in angular form, degrees
Θ_1^+	largest high-pressure area adjacent to Θ_1^- degrees
Θ_2^+	smallest high-pressure area adjacent to Θ_1^+ degrees
N_G	gas-generator speed, rpm
$N_G/\sqrt{\Theta_2}$	corrected gas-generator speed, percent rpm
P_{S2}	static pressure at duct exit, psia
P_{T2}	total pressure at duct exit, psia
ΔP	difference in pressure
P_{TO}	total pressure at duct (separator) exit, psia
W_A	mass flow, lb/sec
Δ_{HP}	difference in horsepower
A_{Min}	minimum particle diameter, in.
R_1	separator hub radius at beginning of swirl field, in.
R_2	collection lip radius, in.
CFM	cubic feet per minute
O.D.	outside diameter, in.
I.D.	inside diameter, in.
T_{T2}	total temperature at duct exit - °R, degrees Rankine

INTRODUCTION

Of all the problems caused by the operation of helicopters and V/STOL aircraft from unprepared sites, a major problem is the erosion of the powerplants by ingested sand and dust. For piston engines, the problem can be handled by cleaning the engine air with conventional filters or separators. These conventional air cleaners are designed for through-flow velocities of between 30 and 50 feet per second; these velocities dictate reasonable flow areas in the case of piston engines. However, for turbo-prop or turboshaft engines, with their vastly increased air requirements, the separator flow areas become restrictive. By ingenious packaging, conventional separators have been successfully installed on some turboshaft-powered helicopters. No such installations have yet been tried on turboprop aircraft. The CV-7A separator described in this report is the result of a program to design an air cleaner with a high flow per unit area that would be more adaptable to turboshaft or turboprop installations.

Initial design efforts in the separator program were directed toward a separator for the T58 turboshaft engine. Since the airflow of the T58 is one-half that of the T64, two T58-type separators with slight modifications were used for the CV-7A separator system.

The CV-7A separator was tested in the facility shown in Figures 1 and 2. This facility was chosen because it is the facility in which all previous separator testing was done; it was readily available and simple to operate. The facility's airflow capacity is dependent on pressure drop across the inlet, but it is nominally equivalent to one-half the T64-GE-8's maximum airflow. Since two separators are required for one T64 Engine, and since each separator operates independently of the other, the facility provided adequate airflow for efficiency testing.

Testing was accomplished by mounting the separator on a CV-7A duct model. The model simulates the flow path of one side of the bifurcated duct required to install the separators in the CV-7A nacelle.

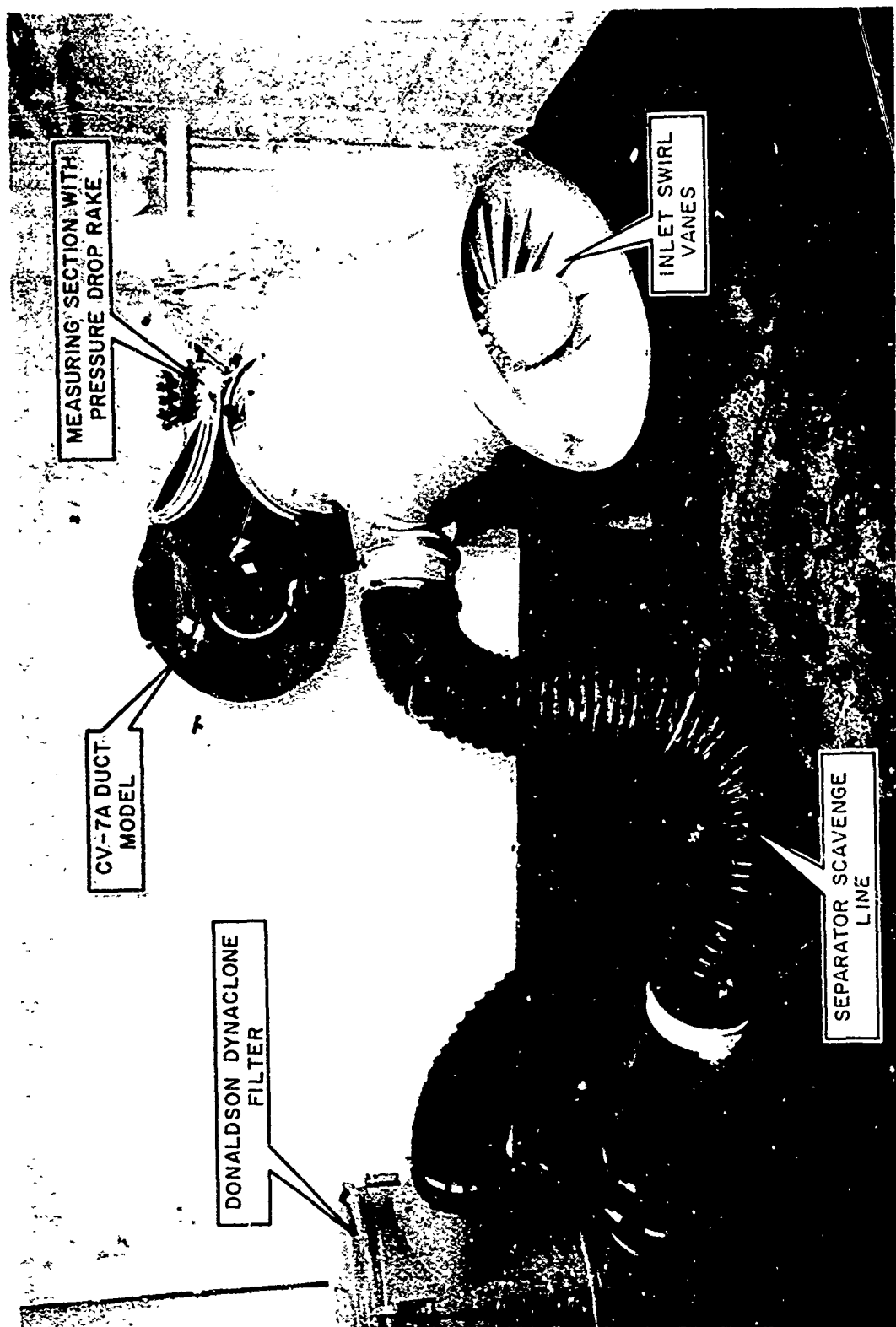


Figure 1. Test Setup of CV-7A Duct Model and Serial Number 2 Separator.

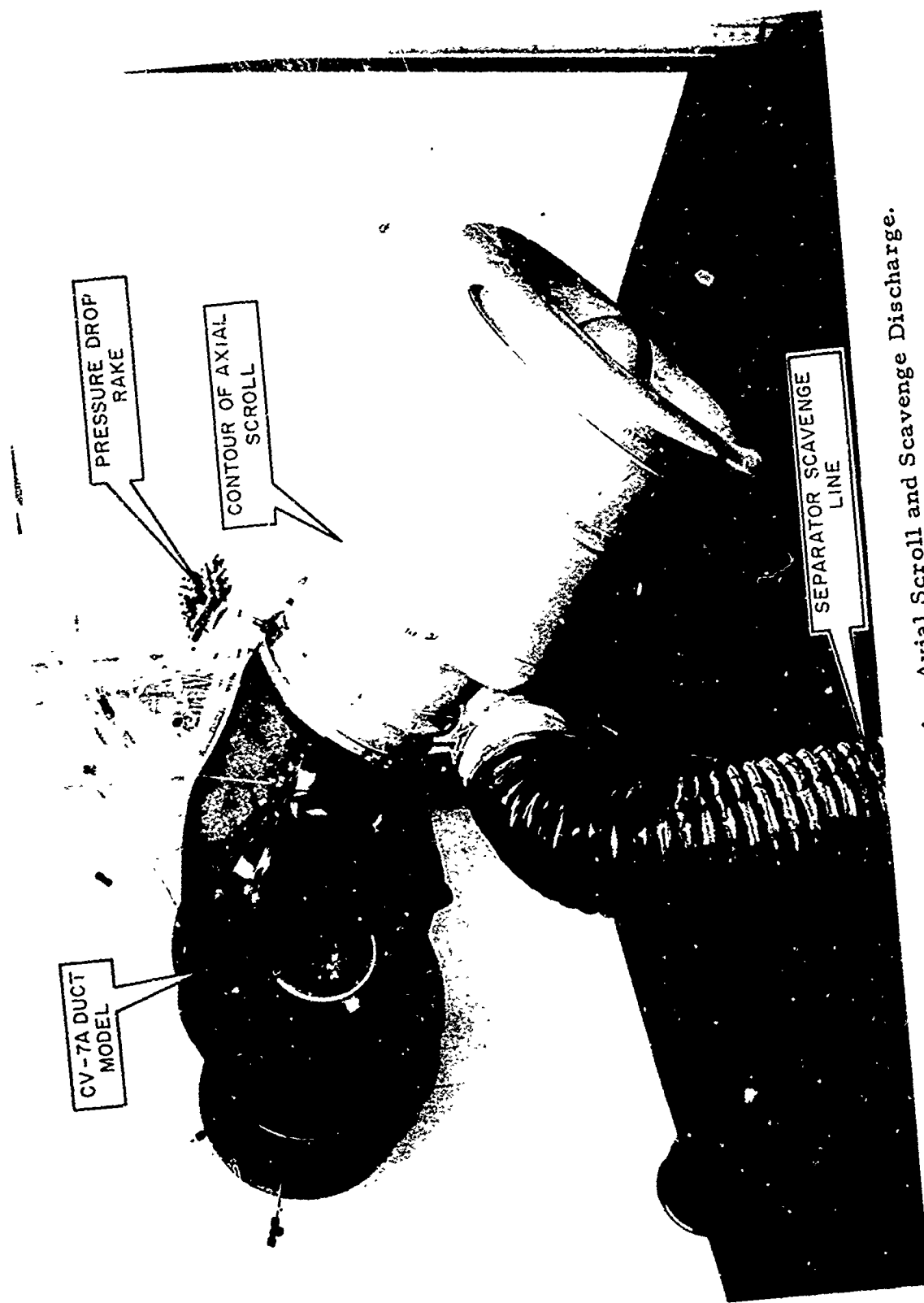


Figure 2. Test Setup Showing Axial Scroll and Scavenge Discharge.

DESCRIPTION OF THE TEST ARTICLE

BASIC SEPARATOR

Figure 3 depicts the T58 separator design and its method of operation. No moving parts are involved in the basic separator operation. As contaminated air is drawn through the separator by the engine, the fixed swirl vanes swirl the air, causing the sand particles, which are much denser than air, to be thrown radially outward. Sand is trapped in the collection scroll, and the clean air passes on downstream, through the exit deswirl vanes and into the engine. In Figure 3, the T58 engine would attach directly onto the discharge end of the separator at the deswirl vane exit.

CV-7A DESIGN

A cross-sectional sketch of the CV-7A separator design is shown in Figure 4. Comparison of Figure 4 with Figure 3 shows the only obvious difference between the two separators is the collection scroll design. In fact, the two separators are aerodynamically identical from the inlet through to the collection lip. Aft of the collection lip, the CV-7A separator has a larger

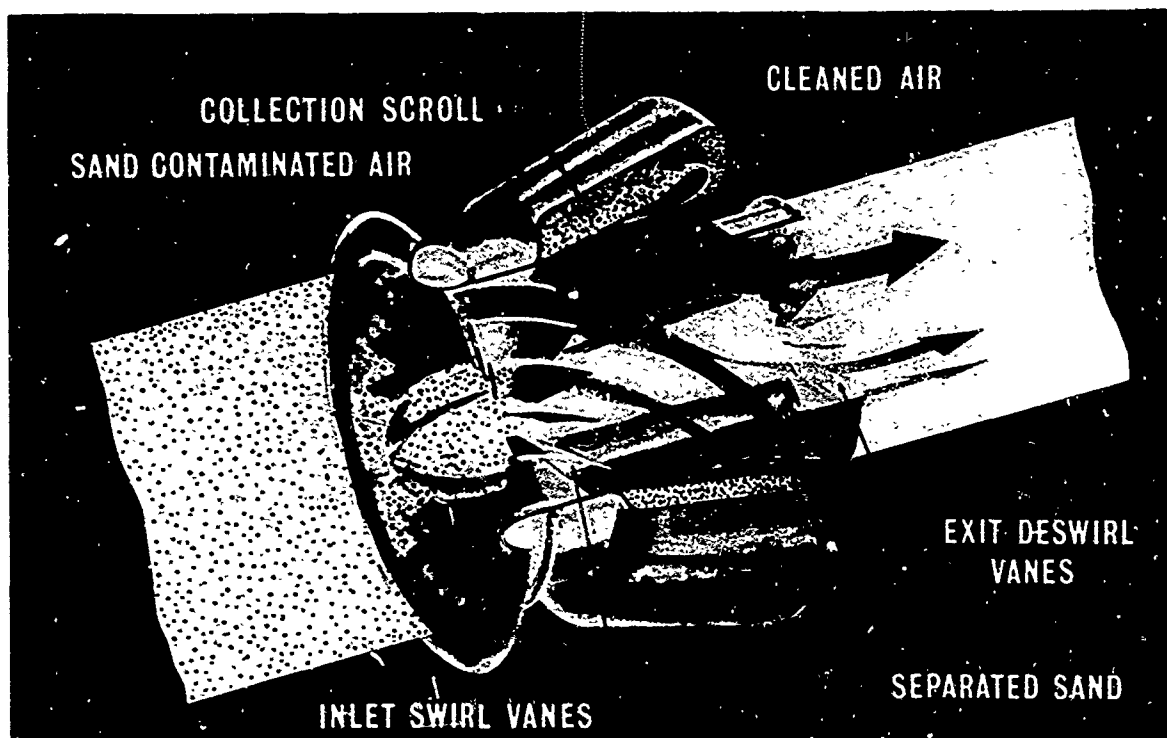


Figure 3. Inlet Separator.

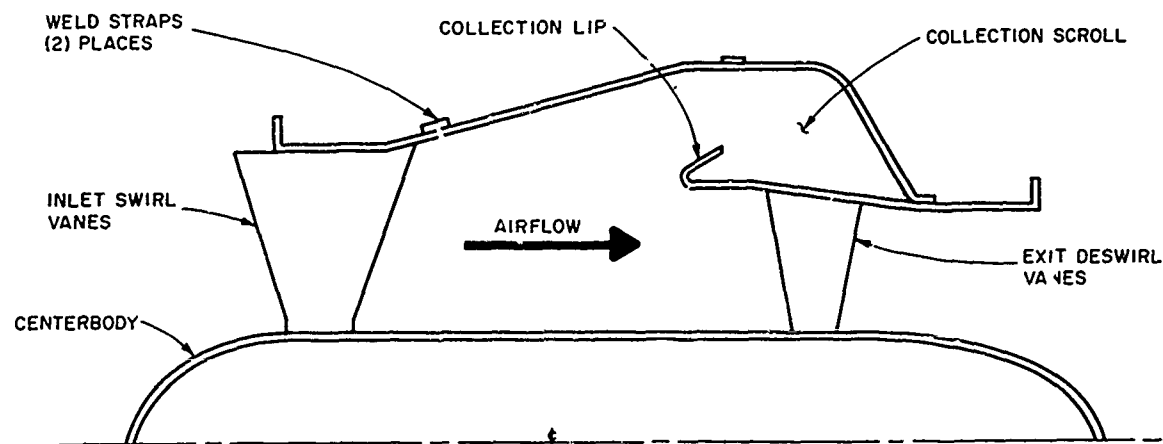


Figure 4. CV-7A Separator Cross Section.

flow area at the exit vanes than the T58 design. Also, the obvious difference in the collection scrolls exists.

The collection scroll design was changed to reduce the overall diameter of the separator. Figure 5 shows that the CV-7A design has a maximum diameter of 17.4 inches. The T58 design has a 22.5-inch diameter. A smaller diameter separator was required to fit the separators in the CV-7A nacelle, without an increase in the nacelle maximum width (projected frontal area). Changing the collection scroll geometry from that of the proven T58 design (Figure 3) was not considered to be a major change, since the function of the scroll is secondary in the sand collection process. As Reference 1 describes, an approximation to the axial collection scroll was tested on a full-scale separator flow model. The two different scroll designs showed no discernible difference in performance.

Two separators were received for the component evaluation. The first one received (Serial Number 1) had butt welds at the two locations in Figure 4 where "weld straps" are shown. Because of the development-type tooling used in the manufacture of the separators, these butt welds had excessive weld burn-through and porosity. This condition was structurally unacceptable and damaging to the internal aerodynamics of the separator.

On the Serial Number 2 separator, the "weld strap" was used in place of the butt weld. No burn-through resulted from this design.

SEPARATOR INSTALLATION

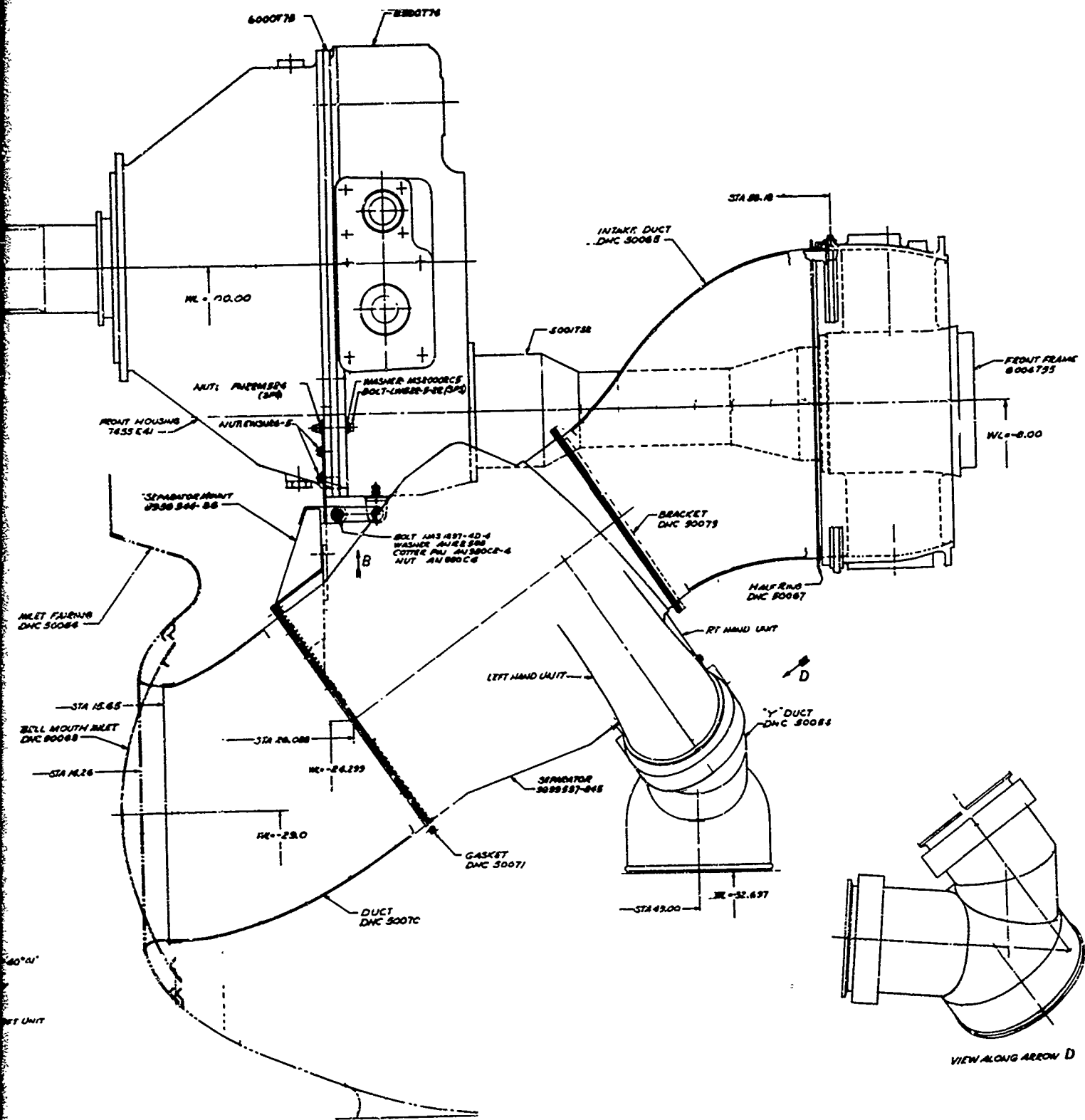
Figure 6 is a partial installation drawing of the separators, showing how the separators are mounted in the CV-7A nacelle. Six degrees of freedom are constrained by the mounting brackets attached from the separator inlet ends to the engine gearbox. A steady mount is provided by the rear section of the intake duct, which is attached to the front frame. This aft portion of the intake duct is bifurcated, changing from two circular areas at the separator discharge to one annular area at the engine front frame face. The portion of the intake duct forward of the separator has been changed from the one circular inlet of the standard CV-7A nacelle to two independent circular inlets as shown in Figure 6. Figuratively, the induction system with the separators is a pair of pants, with a separator in each leg and the waist attached to the engine front frame.

To accomplish the contract requirement of collecting and analyzing the sand separated during the flight test, the two individual separators' scavenge discharge ports are ducted together to form one common "Y" duct, as shown in Figure 6. The common duct is then taken through a sand collection box. Two scavenge fans are placed downstream of the sand collection box to provide suction. Each fan weighs 35 pounds in this flight test configuration.

In a production configuration where there is no need to filter out the sand collected by the separators from the separator scavenge air, a more flight-weight scavenge system could be utilized. Separator scavenge requirements are 600 to 800 cubic feet per minute per separator. Static pressure rise required depends on intake duct recovery, but it should be in the neighborhood of 6 to 8 inches of water. One fan design that would handle the scavenge requirements of both separators is rated at 2000 cubic feet per minute at 8 inches of water static pressure rise. Fan weight is quoted at 6 pounds. Power is supplied by 0.1 pound per second of engine customer bleed air. This fan was specifically designed for sand separator scavenge. The fan blades can be coated with polyurethane to improve erosion resistance. With this fan as a part of the system, a conservative weight breakdown of the separator package would be:

Separators (2 per engine)	38 lbs
Scavenge fan (with damper)	6 lbs
Scavenge ducting (rough estimate)	7 lbs
Bleed air tubing (rough estimate)	12 lbs
	<hr/>
Total (per engine)	63 lbs

No detailed work was done on a production-type scavenge system; therefore, the estimate of scavenge duct and bleed air line weight is necessarily an approximation. The damper on the scavenge fan is required to eliminate reverse flow through the fans when the fans are not being used.



TEST SETUP AND EXPERIMENTAL PROCEDURE

TEST SETUP

Testing of the separator was accomplished with the test setup shown in Figures 1 and 2. The duct model shown in the figures simulates one-half of the bifurcated duct, shown in Figure 6, between the separator and the engine front frame. Since the separators act independently in the CV-7A installation, and since the separator axis is skewed to the engine axis, as shown in Figure 6, the test setup used was felt to be a realistic configuration for component evaluation. Figure 7 is a detailed view of the pressure drop rake identified in Figures 1 and 2. The probe elements are impact tubes spaced 1/8 inch apart on an arm that forms a 4-inch radius arc. This type of probe is required to define the separator exit vane wakes. From measurements with this rake, the pressure drop across the separator is computed as described in Appendix I. The only difference between the procedure of Appendix I and this test was that the rake was placed at seven radial locations instead of six, as described in the appendix. All other aspects of the data acquisition and reduction were the same.

The separators are scavenged by a Buffalo Forge Company Model 4RE 26-inch diameter wheel fan, drawing through the filter shown in Figures 1 and 2 and also through an orifice measuring section not shown. Scavenge flow is adjusted by throttling the fan discharge. During the entire test when scavenge was used, scavenge flow was maintained at a setting to give 6.6% of 100% Military Rated Power engine airflow. This was done to simulate an installed separator system where no fan throttling would be provided.

EXPERIMENTAL PROCEDURE

1. Facility Calibration

The test duct was initially calibrated for flow by installing a calibrated bellmouth on the duct model inlet in place of the separator. The corrected flow, as measured by the bellmouth, was then related to a measurement of corrected velocity head at the duct exit. Figure 8 is the resulting calibration curve. As can be seen from Figure 8, maximum corrected airflow of the facility is in excess of 13 pounds per second. However, as the pressure drop at the inlet is increased (as would occur when the separator is installed), the maximum airflow will drop along the operating line of the fan used in the facility. For this reason, the maximum corrected airflow achieved during the separator component test was 11 pounds per second. Had the pressure loss of the CV-7A separator design been less, the maximum facility airflow would have been higher.

2. Pressure Loss Measurement

Upon completion of the airflow calibration, the Serial Number 1 separator was installed on the duct, as shown in Figures 1 and 2.

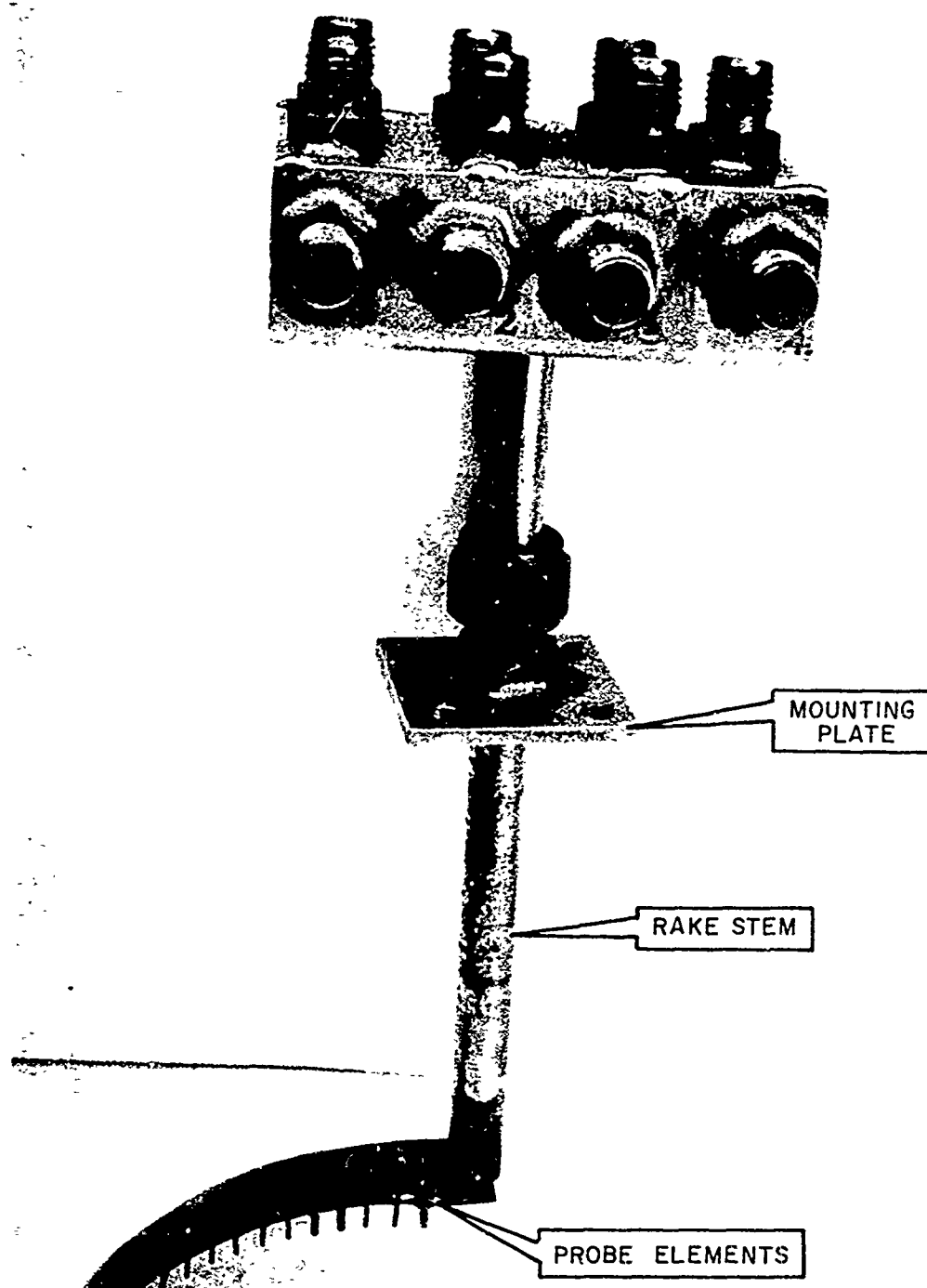


Figure 7. Pressure Drop Rake.

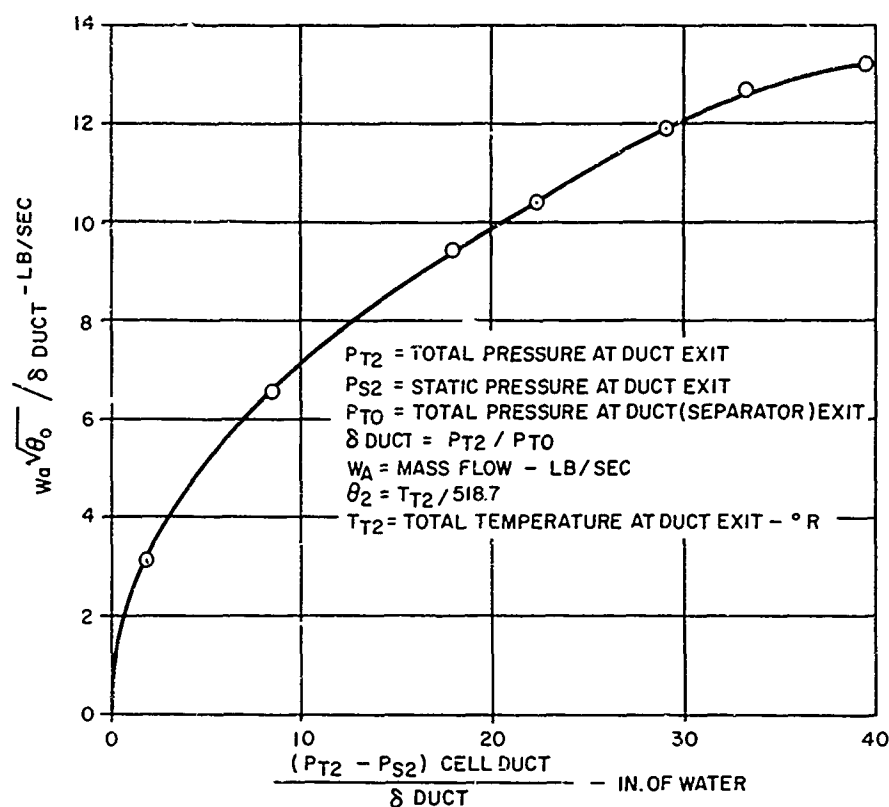


Figure 8. Separator Test Facility Airflow Calibration Curve.

Pressure loss was measured by setting the rake of Figure 7 at seven radial locations between the separator exit annulus' inner and outer walls. Airflow for the pressure loss tests was set by throttling the facility fan discharge. Pressure loss was measured for the separators operating both with and without scavenge airflow through the collection scroll. The Serial Number 2 separator was tested in the same manner.

3. Collection Efficiency Measurement

Separator collection efficiency at discrete particle sizes was measured by hand feeding 10 pounds each of the sands listed in Table I. The amount of sand fed into the separator was weighed on a scale reading to the nearest hundredth of a pound. After the sand was fed into the separator, the weight gain of the filter in Figure 1 was recorded. The filter was then cleaned and reweighed. The scale used to weigh the filter read to the nearest tenth of a pound. Overall accuracy of the test results then (assuming 50% collection efficiency or a filter weight gain of 5 pounds) is $\pm 2\%$. The accuracy was much better than this in most cases, since collection efficiency was greater than 90% in most cases.

TABLE I. TEST SANDS			
Name	Nominal Size Range (microns)	Spread*	Median Dia. by Weight (microns)
AC Coarse	0 to 200	6.66	30
Size P Glass Beads	27 to 53	.355	45
Size N Glass Beads	53 to 74	.331	63.5
Size K Glass Beads	62 to 86	.325	74
#40 Special SiO ₂	210 to 500	.818	355
#1/2 Special SiO ₂	500 to 1000	.666	750
#1/2 Special SiO ₂	1000 to 2000	.666	1500
* Maximum nominal diameter minus minimum nominal diameter divided by median diameter.			

TEST RESULTS

Component test results are presented in Figures 9 through 13. The separator pressure loss curves in Figures 9 and 10 plot computed points resulting from the pressure loss calculation of Appendix I. As noted on the figures, the slope of the line through the data points was taken from previous test results of the T58-type separator. Extrapolation of the data to engine Military Rated Power airflow shows a pressure loss of 11 and 9 inches of water with and without scavenge, respectively. This is the indicated loss across the separator and does not include duct losses between the separator and the engine face or adjustments for losses in the duct which the separator replaces.

Measured component collection efficiency with and without scavenge flow is shown in Figure 11 for the Serial Number 2 separator. These points were measured using the sands described in Table I. As can be seen, these points, which were achieved with a separator main corrected flow of 11 pounds per second, exceed the contract requirements for efficiency at maximum power airflow of 12.5 pounds per second. The separator exceeds the efficiency requirements when operating both with and without scavenge flow. Figure 12 compares the with-scavenge efficiency of the two separators tested. Both separators exceed the minimum requirements, but the poorer quality of the first separator is revealed by its lower collection efficiency.

Table II presents the component efficiency results for the AC Coarse Dust. These data are not plotted on Figures 11 and 12 because the large spread of AC Coarse Dust makes this dust unrepresentative of separator collection efficiency at 30 microns (see page 22 for further data relative to AC Coarse Dust testing).

TABLE II. COLLECTION EFFICIENCY ON AC COARSE DUST*				
Date	Separator Serial Number	Scavenge Flow	Airflow (lb/sec)	Collection Efficiency (%)
8-29-67	1	Yes	9.9	65.8
9-26-67	2	Yes	10.5	70.2
9-27-67	2	No	11.0	55.0
10-5-67	1	Yes	10.4	68.0
* The mass median diameter of AC Coarse Dust is 30 microns.				

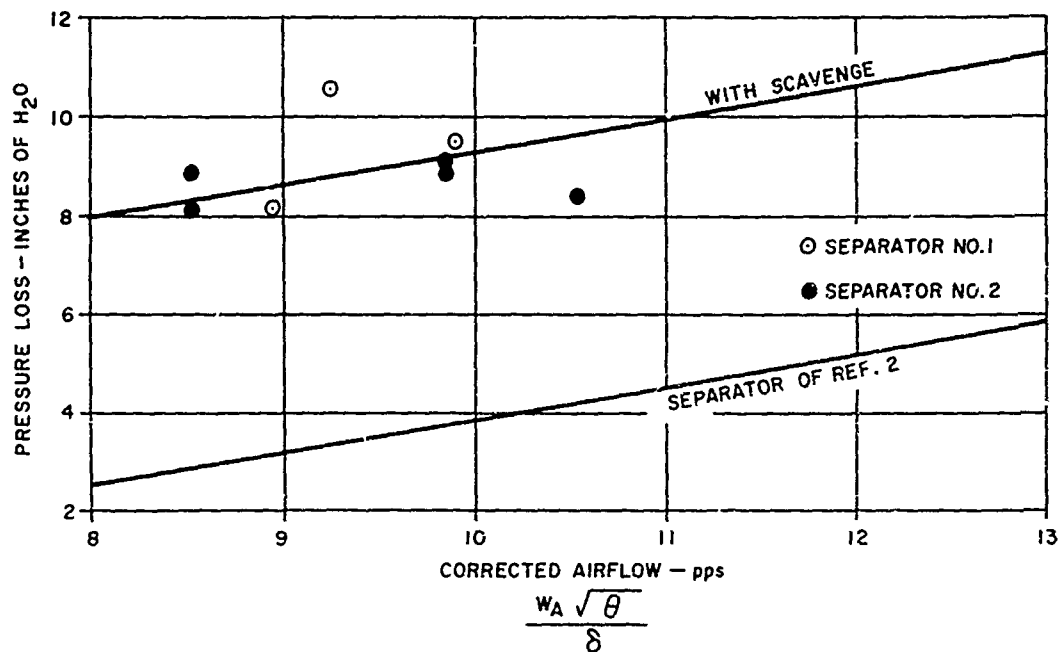


Figure 9. Pressure Loss Across Separator.

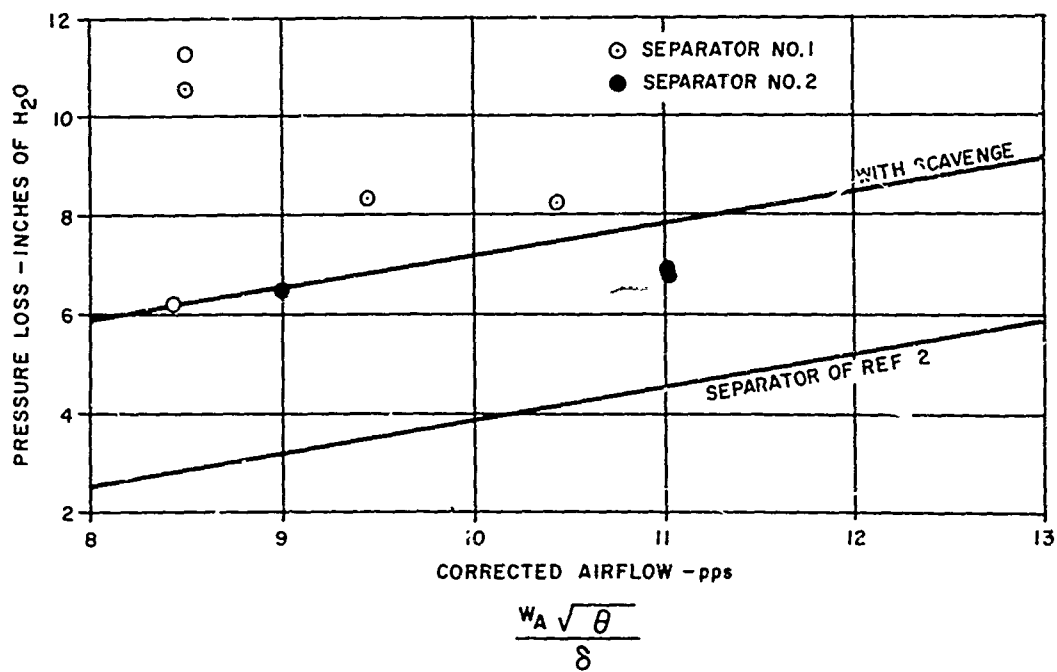


Figure 10. Pressure Loss Across Separator.

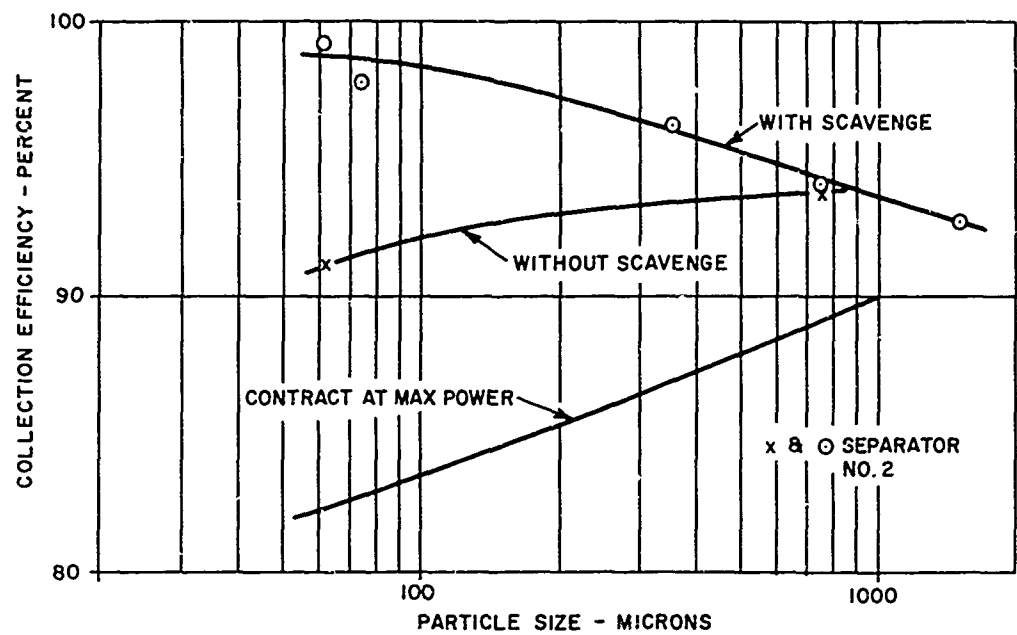


Figure 11. CV-7A Separator Collection Efficiency vs Particle Size.

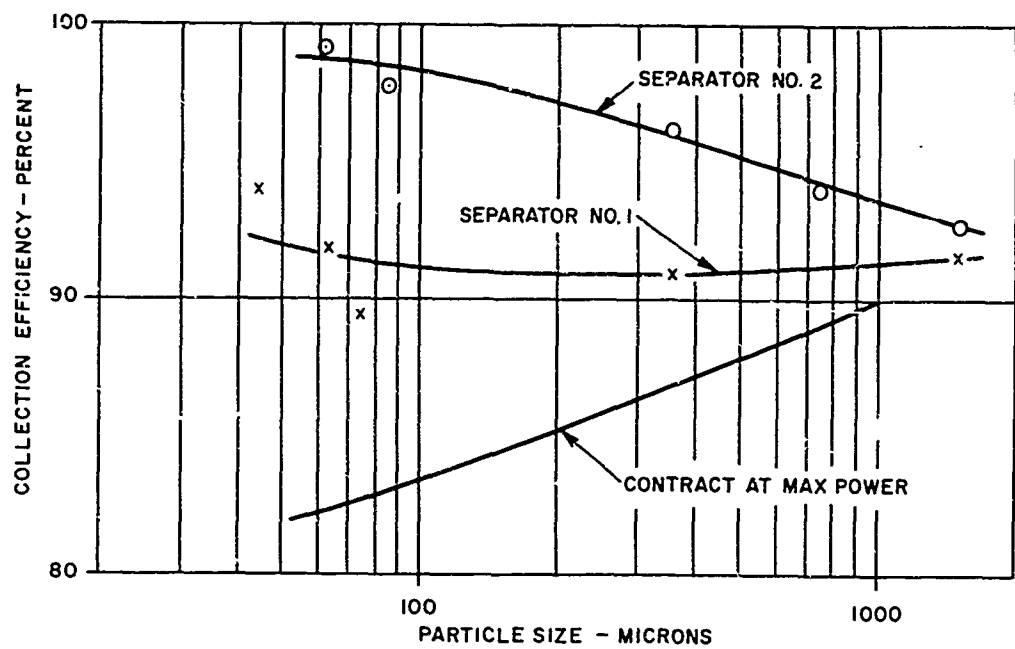


Figure 12. CV-7A Separator Collection Efficiency vs Particle Size.

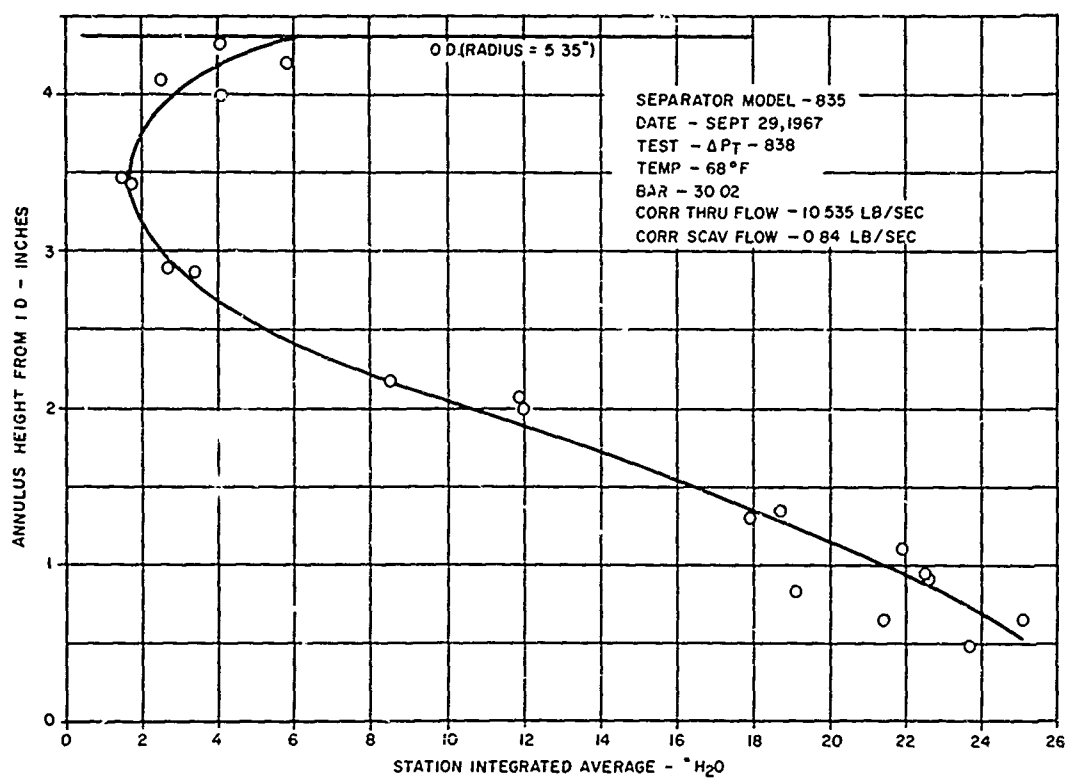


Figure 13. Radial Total Pressure Profile.

DISCUSSION OF TEST DATA

COLLECTION EFFICIENCY RESULTS

As mentioned before, all collection efficiency data were taken with the separator corrected airflow set at 11 pounds per second. This airflow compares with the 12.5 pounds per second which would be seen by this unit when installed in the CV-7A with the engine running at Military Rated Power. To demonstrate the collection efficiency at T64-8 Military Rated Power airflow by testing, expensive facility modifications would have been required. Facility modifications were felt to be unwarranted, since all testing with separators aerodynamically similar to the CV-7A design has indicated a characteristic of increasing separator efficiency as separator flow is increased toward design flow. Since the CV-7A separator exceeded minimum requirements at 11-pounds-per-second corrected airflow, a characteristic just the opposite of all previous separator experience would have to be postulated to conclude that minimum requirements had not been met at 12.5-pounds-per-second airflow. Further, the method of feeding the sand into the separator has been thoroughly explored by tests, as described in Reference 2. Figure 14 shows the pertinent results of these tests. As can be seen, a logical conclusion would be that rate and method of feeding sand have no effect, or at the extreme, give pessimistic efficiency results.

However, it would be of interest to define, by test, the CV-7A separator efficiency versus airflow for several reasons. The collection efficiencies reported for the separator on AC Coarse Dust and on the glass beads below 100 microns are the highest in the writer's experience of working with this separator design, and a better understanding of why this happened might lead to separator improvements. Efficiency of the separator on typical pieces of foreign-object-damage-causing material would also be of interest. However, these items were outside the work scope of the program, and they would not answer the ultimate question of how the separators protect an engine in service. This question can be answered only by flight test evaluation.

EXTRAPOLATION OF DATA TO HIGHER FLOWS

Reference 3 describes extensive component tests of a separator designed for the T58 engine. The T58 separator tested and the CV-7A design are aerodynamically identical from the collection lip leading edge forward. This means that a sand particle in either separator will experience the same forces; i. e., the particle will not know which separator it is in until it is caught in the collection scroll. Figure 15, taken from Reference 3, can be used to extrapolate the results shown in Figures 11 and 12 to higher airflows. Since the efficiencies in Figures 11 and 12 are already quite high, some account must be made of this fact in the extrapolation:

$$\eta_{CV-7A} @ 12.5 \text{ PPS} = 100 - (100 - \eta_{CV-7A} @ 11 \text{ PPS}) \left(\frac{100 - \eta_{c2}}{100 - \eta_{c1}} \right)$$

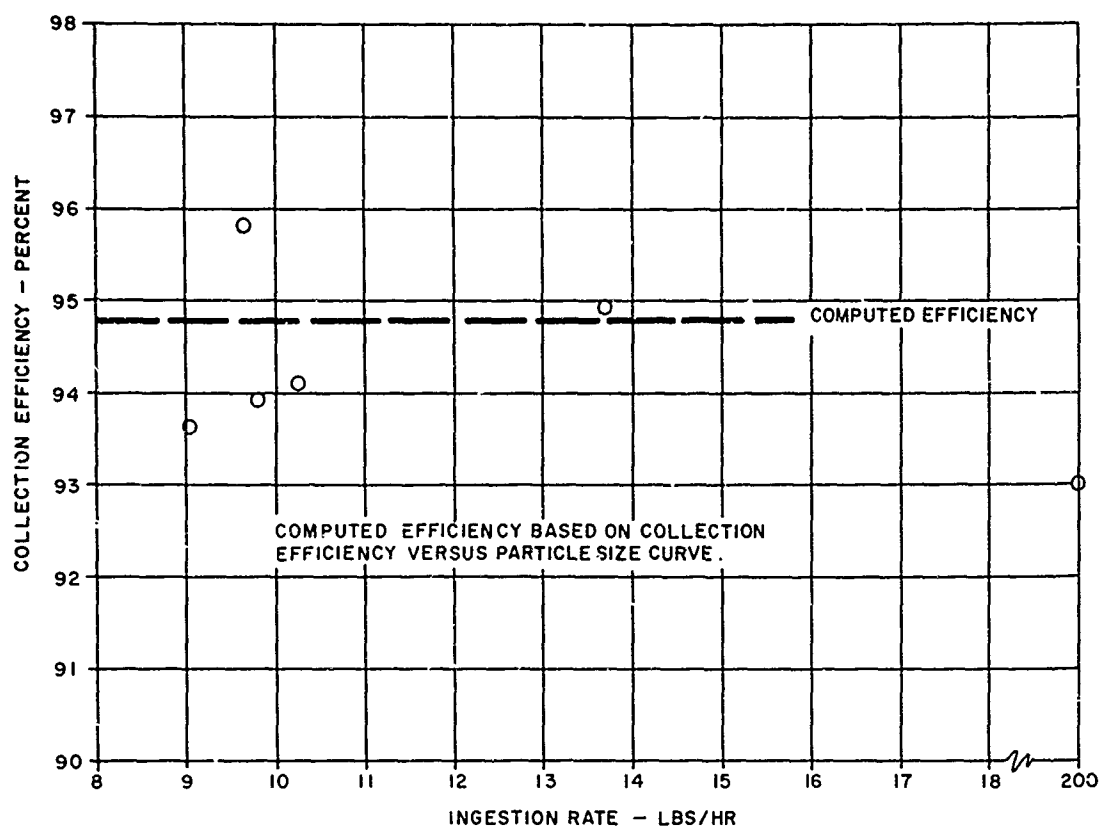


Figure 14. 738 Design Test Efficiency on 0 to 1000 Micron Sand.

where η_c = collection efficiency - percent

η_{c1} = efficiency of T58 design at 11 PPS

η_{c2} = efficiency of T58 design at 12.5 PPS

If this formula is applied to the efficiencies of Figure 11, and if the 0.75-pound-per-second scavenge curve of Figure 15 is used, the efficiencies of Figure 11 change as follows:

TABLE III. SEPARATION EFFICIENCIES		
Mass Median Diameter (microns)	Efficiency at 11 PPS	Efficiency at 12.5 PPS
	Airflow (percent)	Airflow (percent)
63	99.2	99.56
74	97.8	98.8
350	96.2	97.9
750	94.0	96.7
1500	92.7	96.0

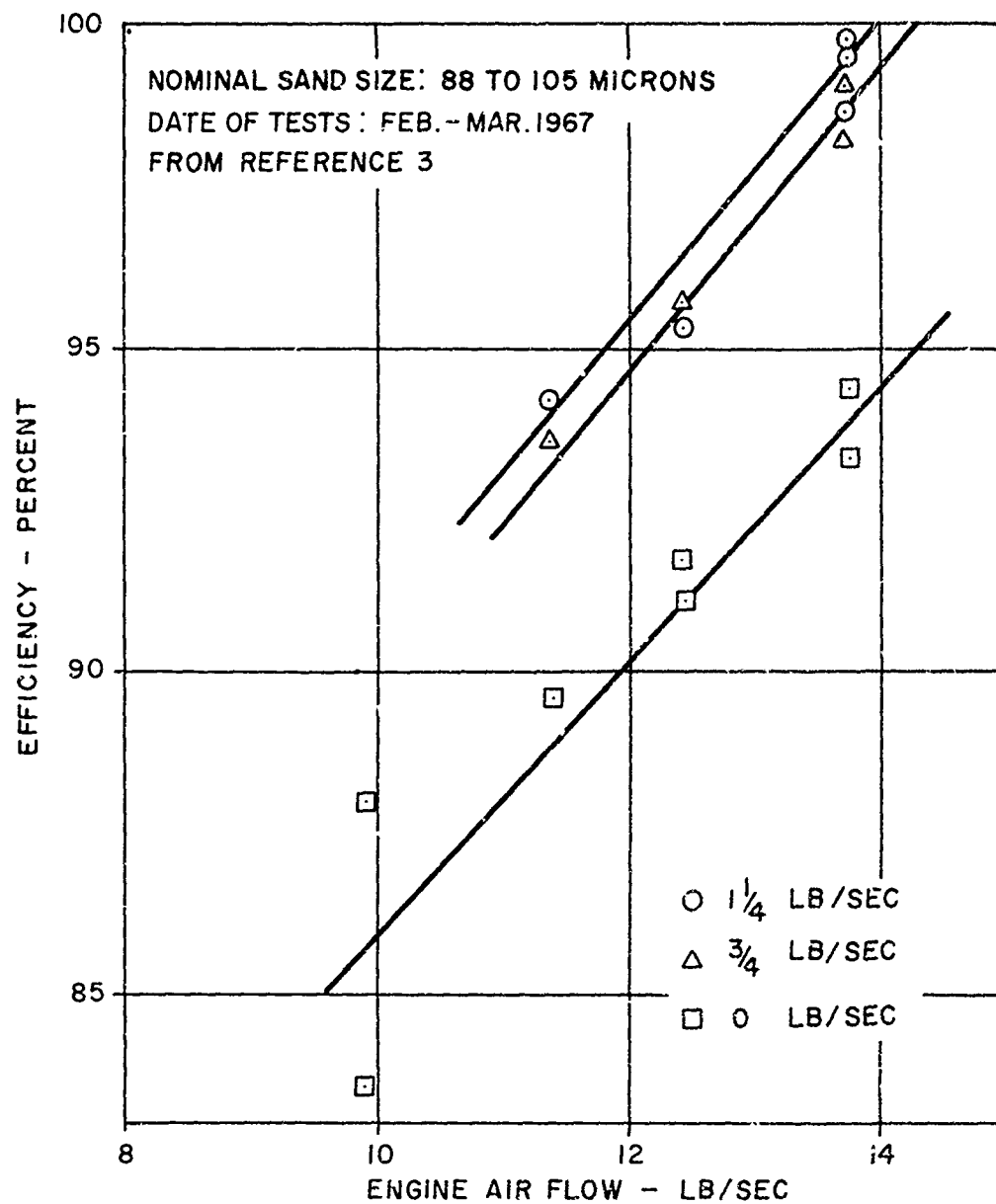


Figure 15. Efficiency of the General Electric Model No. 9899537-738 Inlet Particle Separator as a Function of Engine Airflow.

The figures in Table III are rough approximations, since Figure 15 is for 88- to 105-micron sand and since the characteristic of collection efficiency versus airflow would be expected to be different for different size sands. It is felt, however, that the extrapolation is instructive, at least, qualitatively.

TESTING WITH AC COARSE DUST

Two standard test dusts used in filter separator evaluation are known as AC Coarse and AC Fine. AC Fine has a nominal size range from 0 to 80 microns, and AC Coarse has a size range from 0 to 200 microns. The size distribution of either sand varies within specified limits. If these limits are plotted, Figure 16 results. This figure, which was taken from Reference 2, shows, in addition to the limits of AC Coarse and AC Fine size distribution, a range of cutoff size for a 738-Design separator. This separator is the same separator that was tested in Reference 3.

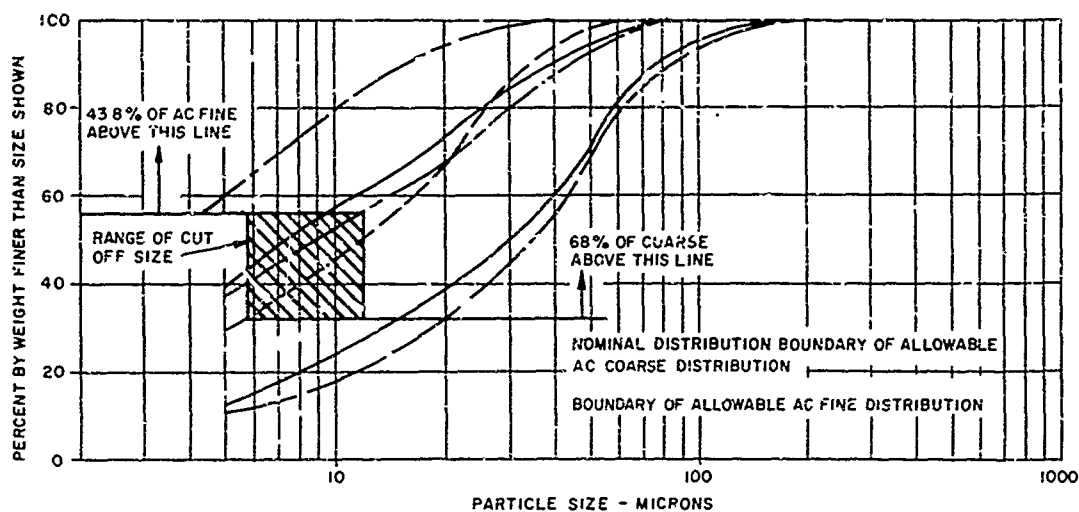


Figure 16. Test Dust Distributions Showing Cutoff Size.

For the 738-Design separator, the component efficiency on AC Coarse, with scavenge, was 68.0%. For AC Fine, the efficiency was 43.8%. If these efficiencies were plotted at the respective mean and median diameter on the efficiency versus particle size curve, an apparent lack of data correlation would appear. This is shown in Figure 17, which is also from Reference 3. The reason for this apparent lack of correlation is that the wide spread of AC Coarse and AC Fine (see page 22) keeps them from being representative of the separator collection efficiency at the mass median diameter of these test dusts. These test dusts are representative of the relative efficiency of one separator design versus another and were therefore used in the component evaluation.

One of the facts that can be generated from the AC Coarse and AC Fine testing is the separator cutoff size. Cutoff size is here defined as that particle size for which the separator efficiency is essentially zero.

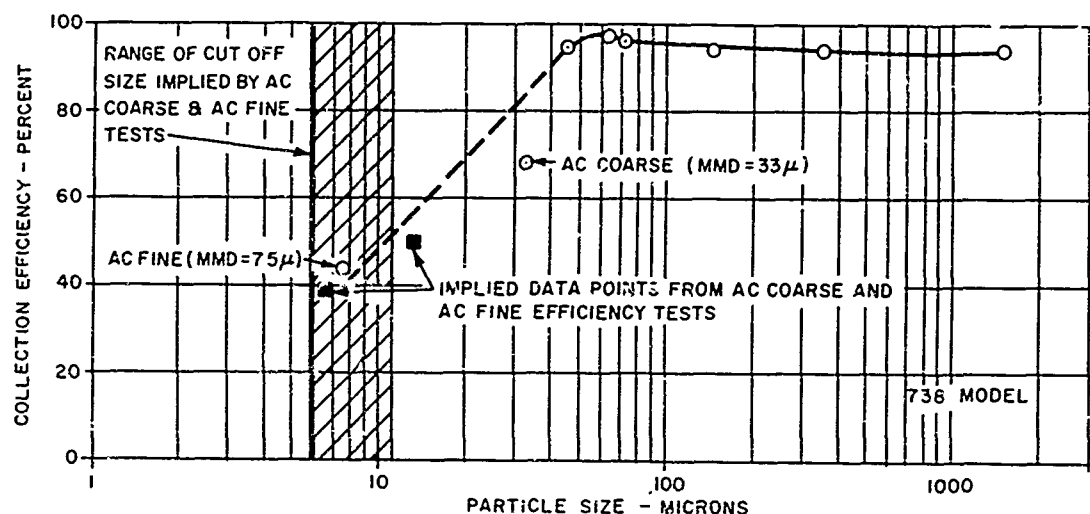


Figure 17. Particle Separator Efficiency with Scavenge.

As shown in Figure 16, if a line is drawn through the AC Coarse distribution limits at 32% of the ordinate and through the AC Fine distribution at 56% of the ordinate, the two lines overlap between 5.8 and 12 microns. The implication of these lines is that (for AC Coarse, for instance) 68% of the AC Coarse was caught by the separator and 32% was passed. If 100% efficiency is assumed on the upper 68% of the AC Coarse distribution, then the separator caught none of the sand between 20 and 5.8 microns. For the AC Fine test results, the implication is that none of the dust between 12 and 4.3 microns was caught. Since there was no precise measurement of the exact size distribution for the two sands used, the range where the horizontal lines of Figure 16 overlap is the range of sizes where the separator efficiency drops to zero.

Another piece of data that can be derived from the AC Coarse and AC Fine tests is the implied efficiency points as shown in Figure 17. These points are significant because the lowest size of test sand available in quantity is governed by the minimum standard sieve size of 37 microns. These points are computed by applying the efficiency curve of Figure 17 to the nominal AC Coarse and AC Fine distributions of Figure 16 and by computing the efficiency that is required on the dust below 45 microns, in order to achieve the efficiencies as measured by testing. As Figure 17 shows, these implied efficiency points provide a more reasonable extrapolation to the lower size ranges than the AC Coarse or AC Fine results, and they provide an estimate of separator efficiency below 37 microns.

Similar exercises could be applied to the CV-7A design, with similar results expected due to the similarity of the two designs.

PRESSURE LOSS TESTS

The primary purpose of the component tests was to determine the collection efficiency of the separator. Pressure loss data were to be taken during the engine testing of the separator, which is the only true measure of the effect of the separator on installed engine performance. However, engine testing was not included as part of the scope of modification No. 1 to the contract and, therefore, was not accomplished. However, in an effort to provide meaningful estimates, pressure loss measurements were made during the component test to get an approximation of what engine results could be expected and to allow for modifications if the pressure loss was too high.

The special rake shown in Figure 7 was used for the pressure loss measurement because the separator exit vane wakes must be accounted for in the pressure loss computation. The method is described fully in Appendix I. In essence, the method of pressure loss computation is to integrate across the maximum number of vane spacings at each radial immersion of the rake. The result of such an integration is shown in Figure 13. Since the vanes are closer together at the inner diameter than at the outer diameter, five data points result from the inner diameter immersion and only two at the outer diameter.

As Figure 13 shows, the radial pressure profile aft of the separator is significant, showing a radial distortion of 5.9%. This plot, which shows the data corrected for probe calibration, was used to get the average pressure loss across the separator. A further correction which could be applied to the data is to average Figure 13, not on an area weighted basis but on a mass flow weighted basis, since this is the average pressure that the engine really senses. If this were done, the pressure drop would be less than the area weighted integration, because mass flow is proportional to the square root of the total to static pressure difference. Since no static pressure gradient is assumed for the flow aft of the separator exit vanes, more weight would be given to the high total pressure region of Figure 13, resulting in a lower separator pressure loss. For example, if the lower 20% of the exit annulus is assumed to be stagnant as Figure 13 suggests, then the pressure drop based on equal areas across the upper 80% of the annulus is 4.65 inches of water, not the 8.58 inches of water as shown on Figure 13.

Distortion caused by the separator is not expected to be an operational difficulty. The T58 separator gives distortion at its exit similar to that shown in Figure 13. This design mounts directly onto the T58 front frame and has been run on the engines. Reference 3 describes such an engine test. No adverse effects, except for the expected power loss, were experienced as a result of the addition of the separator.

It should be noted that the profile of Figure 13 will dissipate somewhat in the bifurcated duct between the measurement plane and the T64 engine. Appendix II describes the results of preliminary duct/separator tests to assess recovery and distortion. These tests showed that the duct/separator combination gave a circumferential distortion index that was within engine specification limits, and that radial distortion exceeded specification limits by 1.0% at 92.5% speed.

DESIGN IMPROVEMENTS

Collection efficiency of the CV-7A separators was higher than expected, and no effort in improvement of this aspect of separator performance is warranted. However, the pressure loss across the separator could be improved. Appendix III describes one possibility which shows promise, but it has not yet been thoroughly explored.

As a design improvement to the present hardware, attention should be directed to the exit vane cascade. From previous experiences with the separator design, it is known that the exit vane has a high loss coefficient. Figure 18 plots the predicted and measured loss coefficients for the exit vane cascade as taken from Reference 5, which describes a model test. Because this fact was known at the time of the CV-7A design, the exit vane cascade flow area was increased in the CV-7A design 18% over that of the T58 separator. In spite of this, the measured losses were high for the CV-7A separator. This would suggest that exit vane restaggering or re-cambering might be in order. Other things that might be tried are slotting

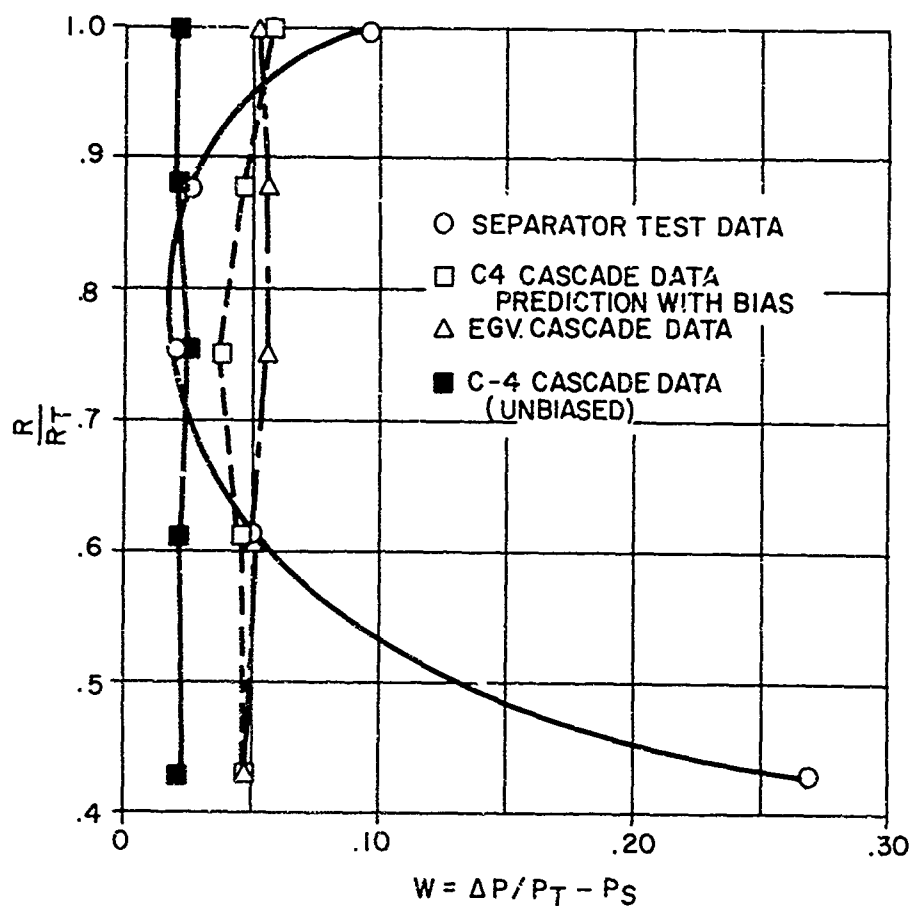


Figure 18. Inlet Separator - Exit Guide Vane Losses vs Radius Ratio.

the vanes or further opening up the flow area. All of the above changes could be accomplished without changing the separator envelope.

All of the above-suggested changes would be tried only after a detailed evaluation of the present component data and after an engine test indicated a definite need for pressure loss improvement.

CONCLUSIONS

1. Contract requirements for separator efficiency were exceeded by the CV-7A separator described in this report. (See Figures 11 and 12.)
2. Based on bench test pressure loss measurements, the installed power loss due to the addition of the separator is marginal relative to the 3% contract limit.
3. An increase in the separator exit vane cascade inlet area and a change in exit vane stagger angle would reduce separator pressure loss. However, no estimate of the amount of pressure loss reduction that is possible can be made because of the lack of available test data due to the limited contract work scope.
4. Weight of two separators required for one T64-GE-8 engine is 38 pounds. This weight is exclusive of scavenge fans and scavenge ducting, which vary in weight depending on installation requirements. Fan size and weight depend on aerodynamic restrictions designed into the scavenge system because of installation requirements. (See Separator Installation, page 8.)
5. Separator efficiency without scavenge exceeds minimum contract requirements for separation efficiency (see Figure 11).
6. Based on component tests of a similar separator with a model of the inlet duct required to accommodate the CV-7A separator, engine inlet circumferential distortion is expected to be within engine specification limits (see Figure 28). Compressor face radial distortion is expected to remain within limits at all compressor speeds except at 92.5% corrected speed where limits are exceeded by $\approx 1\%$. This is not expected to cause serious difficulty, based on previous engine-separator experience.

RECOMMENDATIONS

Based on the bench test results, and in light of the continuing need for inlet protection for V/STOL aircraft, the following recommendations are made:

1. Reduce the separator pressure loss by including the latest design techniques in the current separator envelope. More information about separator pressure loss characteristics and design improvements can be expected from future separator development programs.
2. Verify the separator installed pressure loss by factory engine test.
3. Allow adequate space in new V/STOL aircraft for inlet protection.

LITERATURE CITED

1. Duffy, R. J., Particle Separator Development Program,
General Electric Company, TM65SE803, March 1965
2. Duffy, R. J., Effect of Sand Ingestion Rate on Separator Collection Efficiency as Determined by Component Test,
General Electric Company, TM66SE239, November 1966
3. Elsasser, T. E., The Navy's Inlet Protection Program at the Aero-nautical Engine Department. Paper 67-ENV-4
Presented at the 7th Annual National Conference on Environmental Effect on Aircraft and Propulsion System
4. Duffy, R. J., Component Performance Testing of a 10,000 CFM Particle Separator, -738 Design, General Electric Company, TM66SE246, December 1966
5. Isbell, J. B., Compressor-Inlet Particle Separator Performance,
General Electric Company, TM65SE100, January 1965

The appendixes describe aspects of separator test procedure and development that are directly applicable to the CV-7A separator program. This information is not included in the body of the report in the interest of giving a concise account of the CV-7A program. The information is necessary to a detailed understanding of separator test procedure, duct-separator distortion levels, and potential separator improvement.

Appendix I describes the specialized method of measuring separator pressure loss so that the effects of vane wakes at the separator exit can be accounted for. Appendix II describes testing of a model of the CV-7A separator duct in conjunction with a separator similar to the CV-7A design. This test was run at the beginning of the CV-7A design program to determine if excessive pressure drop or distortion would occur due to the separator installation. Appendix III presents component model test results of several improvements to the basic separator design. This is appropriate to an evaluation of the potential of improving the CV-7A design by techniques not apparent to those unfamiliar with the separator characteristics.

APPENDIX I PRESSURE PROFILES

Reference to Figure 19 shows that as the wake rake is moved along a radial line, the arc of the rake spans a varying number of vanes and is at different radial immersions for a given stem immersion. Figures 20 through 25 plot the set of readings obtained from each probe element of the wake rake for a certain configuration of the separator. Integrating these plots to get the pressure of each immersion would be incorrect because of the geometry of the wake rake.

To integrate the wake rake data correctly, a 2X diagram of Figure 19 was made. A distance of 2 pitch from the rake stem along the arc of the wake rake was measured. Then, from 2 pitch-out back to 1 pitch-out was measured. Since the probe element spacing was known, the measured distances were converted to number of probes, and the wake rake plots were integrated from 2 pitch to 1 pitch from the wake rake stem. This was done for each immersion, and the results were plotted at the radial immersion of the midpoint of the arc between 2 pitch-out and 1 pitch-out from the wake rake stem.

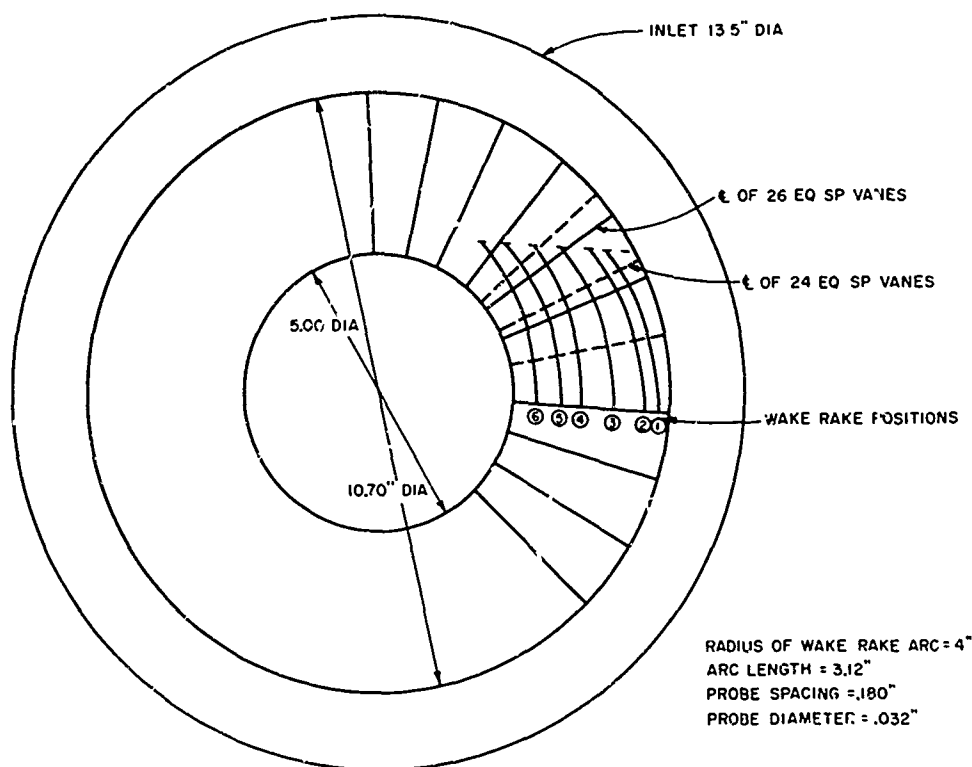


Figure 19. Wake Rake Span Across Exit Vane Spacings.

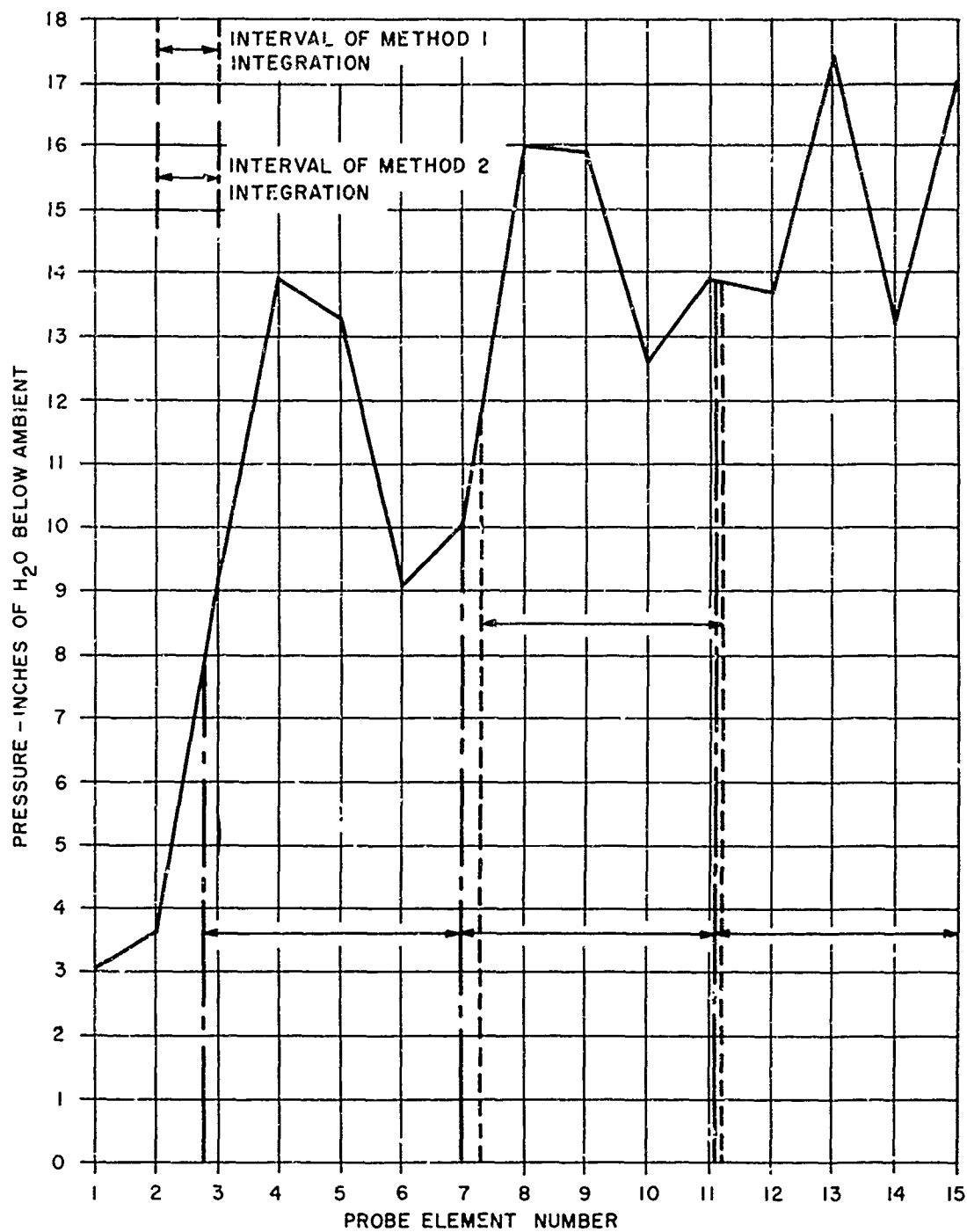


Figure 20. Wake Rake Readings - Immersion 6.

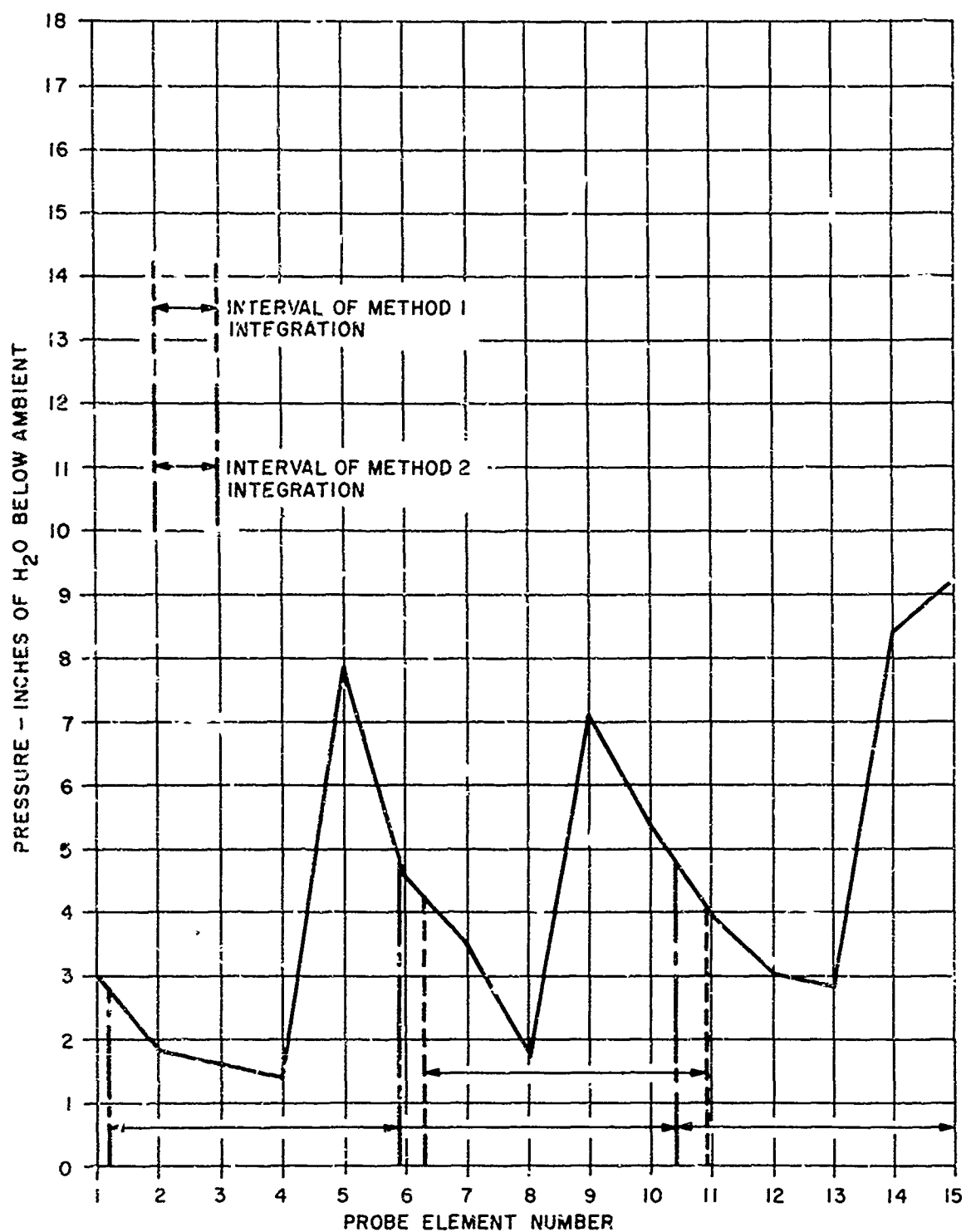


Figure 21. Wake Rake Readings - Immersion 5.

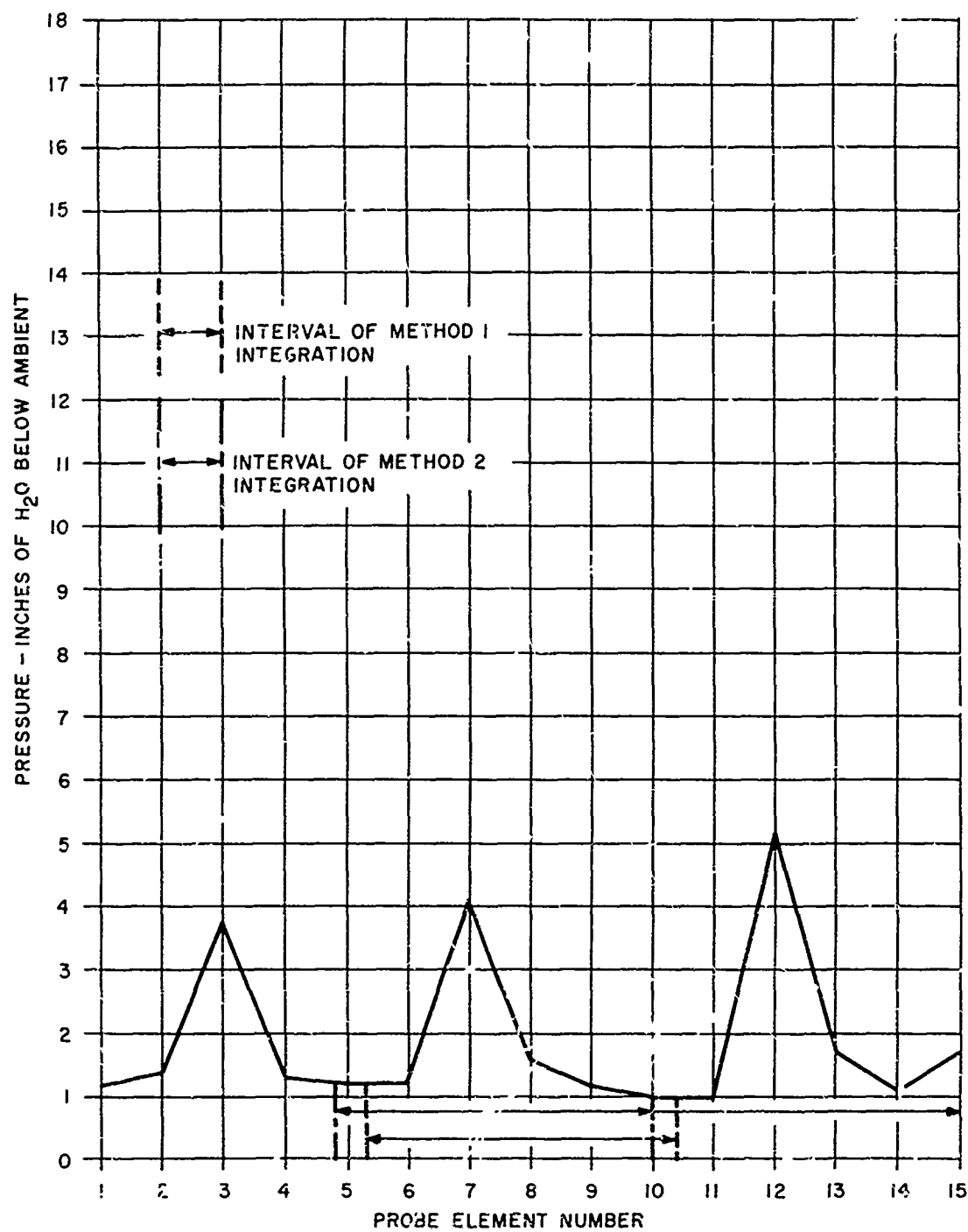


Figure 22. Wake Rake Readings - Immersion 4.

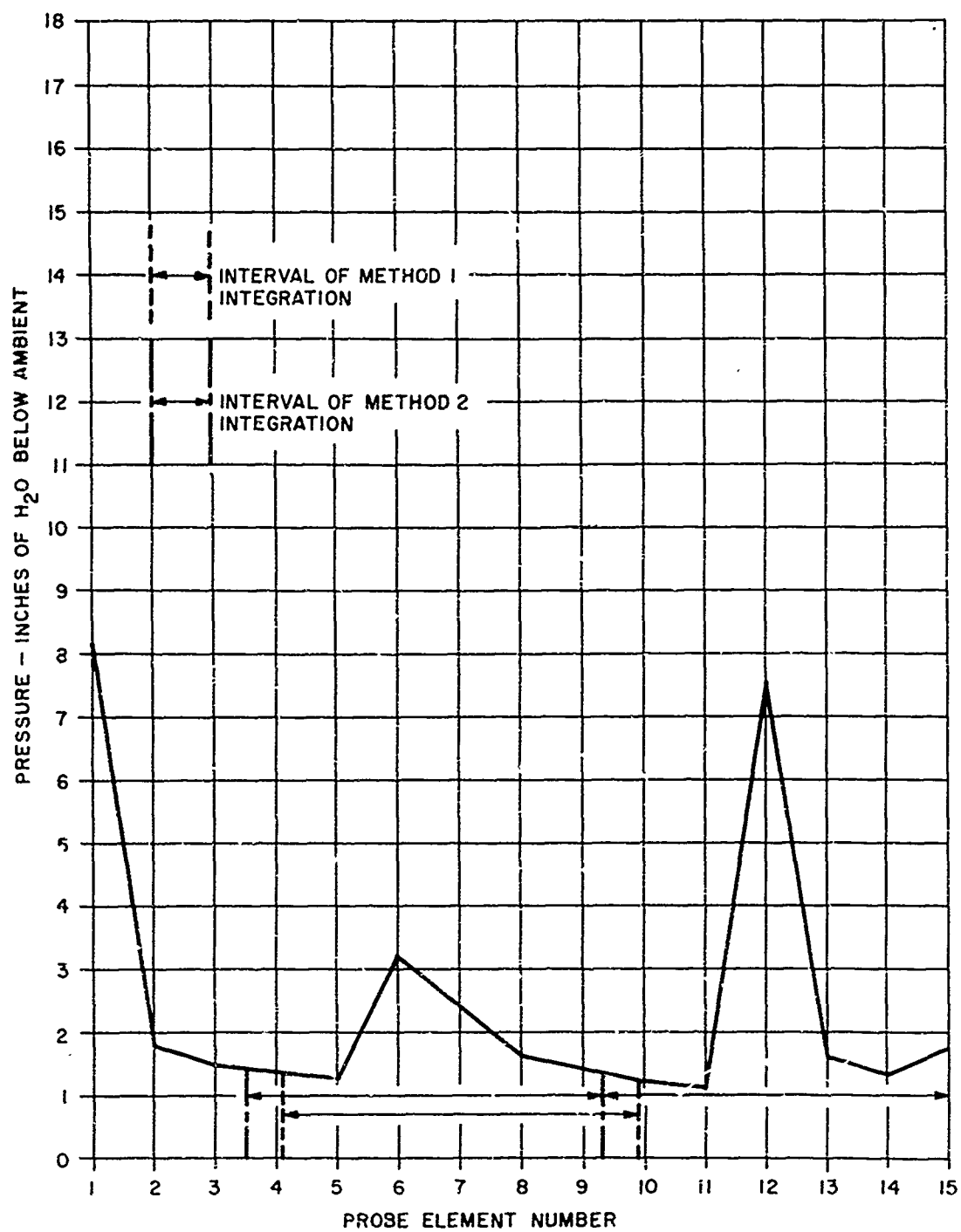


Figure 23. Wake Rake Readings - Immersion 3.

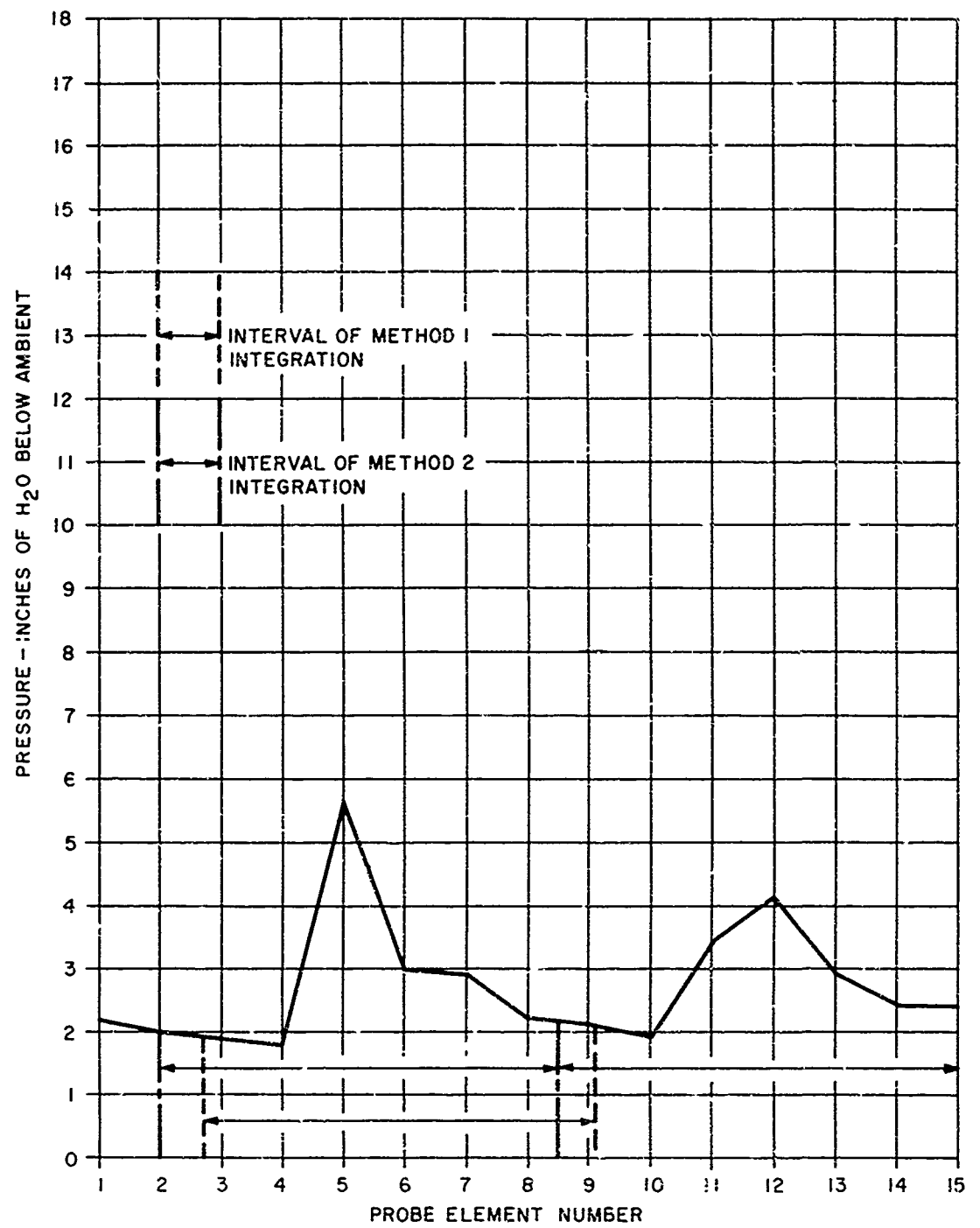


Figure 24. Wake Rake Readings - Immersion 2.

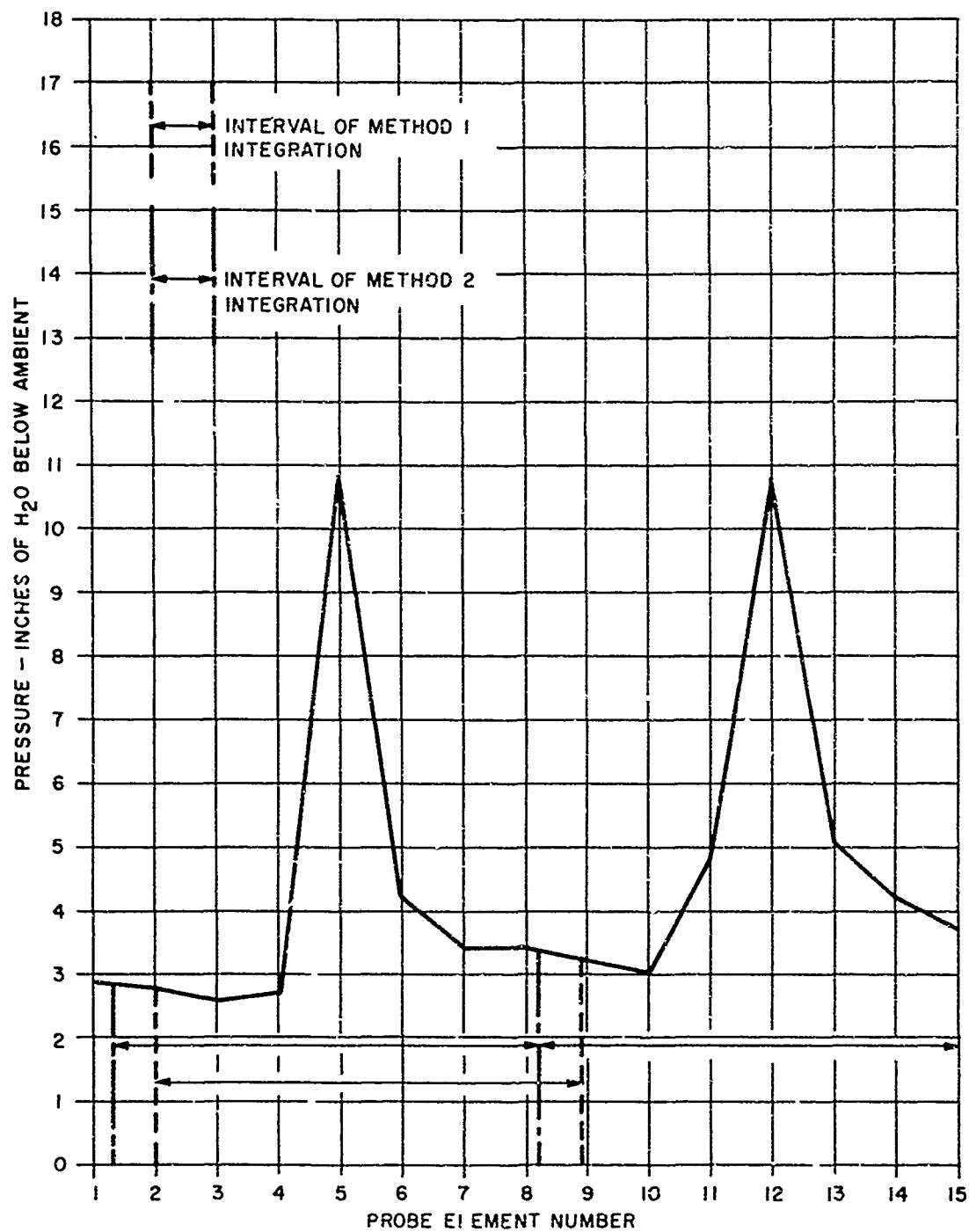


Figure 25. Wake Rake Readings - Immersion 1.

One of the results of the above method is that only a small number of the probe elements are used at each immersion in arriving at the total pressure at each immersion. Another method of integrating would be to integrate across the maximum integral number of vane spacings spanned by the wake rake arc at each immersion. Doing this results in three pressure-drop readings at the hub and two pressure-drop readings at the outer diameter for the configuration shown. For the CV-7A, because a reading was taken closer to the hub, five points were computed for the hub immersion.

The results of the two methods for the same traverse are plotted in Figure 26. Of course, at one immersion of the wake rake stem, the arc, spanning across 3 pitch, is at three different radial immersions (see Figure 19); therefore, the results of integrating across 3 pitch at the hub are plotted at three different immersions.

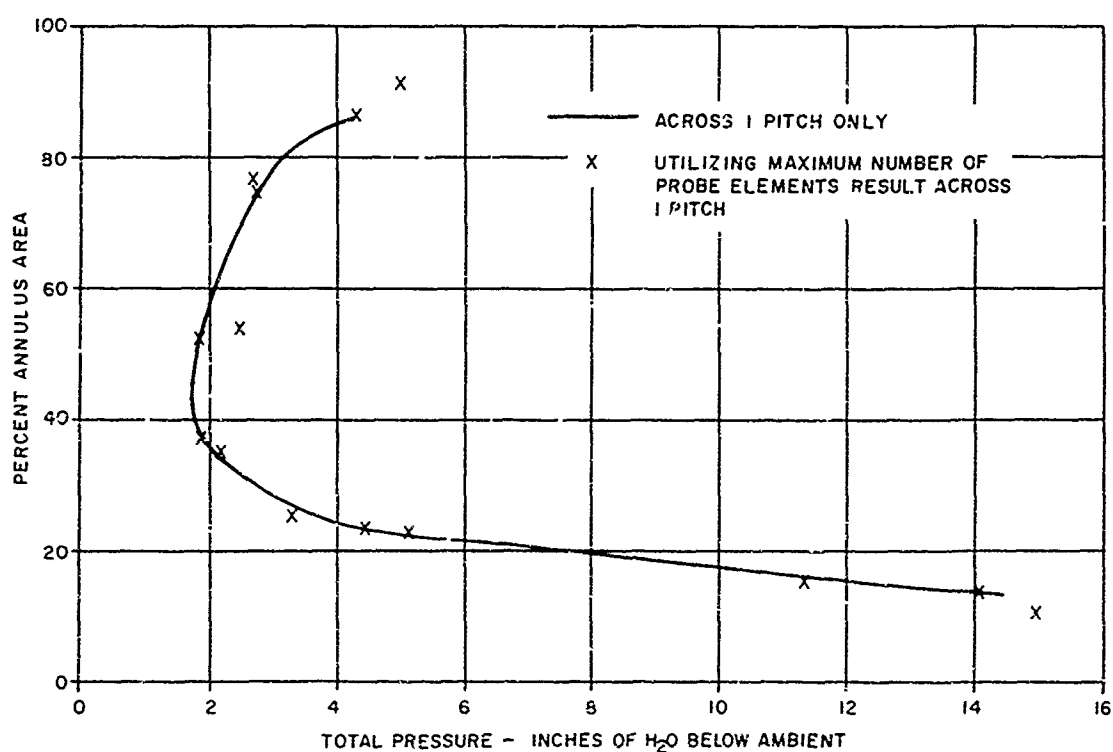


Figure 26. Wake Rake Traverse by Two Different Integration Procedures.

APPENDIX II
PRELIMINARY EVALUATION OF DUST-SEPARATOR
PRESSURE LOSS AND DISTORTION

I. INTRODUCTION

This appendix presents the detailed results of an airflow test program, carried out on a full-size CV-7A/T64 model inlet duct and separator, in order to determine radial distortion, circumferential distortion, and pressure recovery.

The particle separator installation on the CV-7A aircraft incorporates two separators mounted side-by-side with individual associated ducting between airframe and engine inlets. Since the separators are inclined relative to the engine center line, the airflow is distorted through two planes prior to entering the engine.

Testing was carried out on one separator and ducting system, since results were assumed to be representative of a full annulus on a mirror image basis. Separator model number 9894537-573 was used, since the CV-7A design was not yet available.

II. CONFIGURATION

The test components were assembled and mounted in the facility in a manner similar to that shown in Figures 1 and 2.

The assembly consisted of a bellmouth and separator, test duct, measuring duct, and dump section, mounted in that order, with the dump section attached directly to the facility flange. No support was required by the separator because of the adequate rigidity of the duct assembly.

The separator was quickly detachable using a Marman-type clamp; for three tests, it was removed and replaced by a standard T58 bellmouth.

Instrumentation was as shown in Figures 42, 43, and 44.

The downstream end of the separator, which was originally mounted directly onto the T58 front frame, was fitted with a wooden after-body plug to provide an improved profile for flow exiting from the separator.

III. INSTRUMENTATION

Instrumentation of the test duct consisted of a rotatable rake assembly and wall static tapings.

The rake assembly was rotatable through a total of 180 degrees, with provision for locking at any intermediate position. Six total probes

and one static probe were incorporated into the assembly, with the pressure measuring plane occurring at the simulated engine intake (Figures 42, 43, and 44).

Twenty-two static probes were employed in four groups of four and two groups of three. With the exception of one group of three, in which the static probes were widely spaced circumferentially near the measuring plane, the remainder were axially located at pitches between 1 inch and 1-1/4 inch, at points of most severe duct radii.

IV. DISCUSSION

The pressure recovery value of 97.75% at a flow of 25 lb/sec had to be extrapolated from test data, since the facility was incapable of providing this flow. Relating pressure recovery to power loss indicates a 4.2% loss in power at Military Power Rating. This, it is anticipated, would be improved during operation of the hardware, since the deHavilland loft lines result in an increase in overall length and a change in radii, resulting in better flow turning characteristics.

Distortion characteristics, both radial and circumferential, show a marked drop in performance over the lower 50° to 120° of the duct, the area of most severe flow turning.

Figure 27 shows the maximum loss in pressure recovery at 25 lb/sec (12.5 lb/sec per separator system) with and without the separator fitted, and it also shows a comparison of the existing and original duct configurations. A 3% power loss is equivalent to a 98.15% pressure recovery, which the analysis has shown to be exceeded by 0.4% at 25 lb/sec airflow.

Figure 28 shows the circumferential distortion index calculated by using the parameter:

$$N_c = \left[\frac{P2 \text{ Max} - P2 \text{ Min}}{P2 \text{ Ave}} \right] \sqrt{\frac{\left(\frac{\theta_1^-}{90} \right) \left(\frac{\theta_1^+}{\theta_1^+ + \theta_2^+} \right) \left[\frac{\left(\frac{\theta_1^-}{90} \right) \left(\frac{\theta_1^+}{\theta_1^+ + \theta_2^+} \right) + \left(\frac{\theta_1^+}{90} \right) \left(\frac{\theta_1^-}{\theta_1^- + \theta_2^-} \right) \right]}{2}}$$

where:

- P2 Max = the highest total pressure in the sectors under consideration at a given diameter.
- P2 Min = the lowest total pressure in the sector under consideration at the same diameter as P2 Max.
- P2 Ave = the area weighted average total pressure at the same diameter as P2 Max.

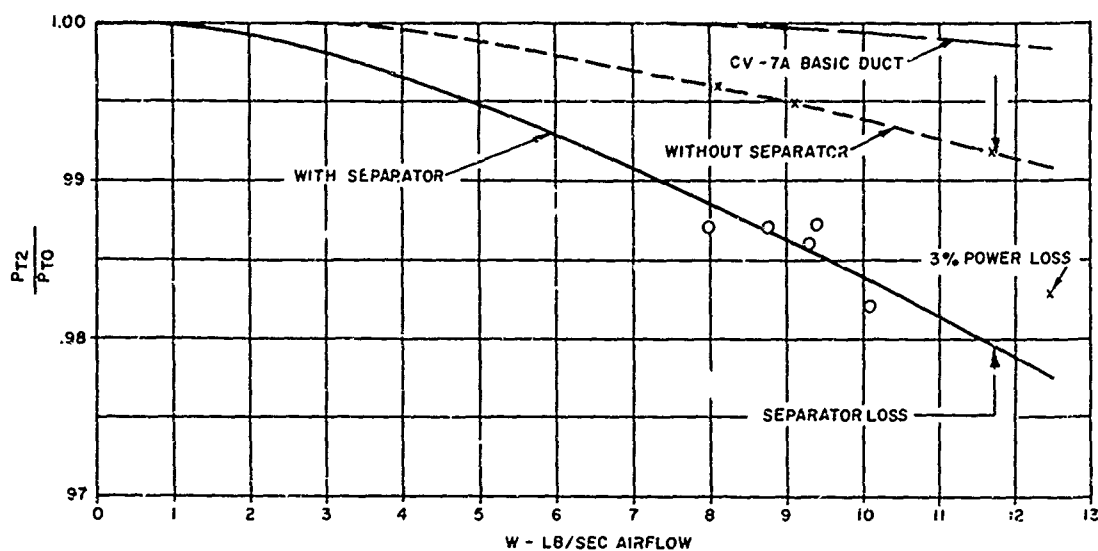


Figure 27. CV-7A/T64 Inlet Duct - Pressure Recovery for Basic Duct and Separator Installation Configuration.

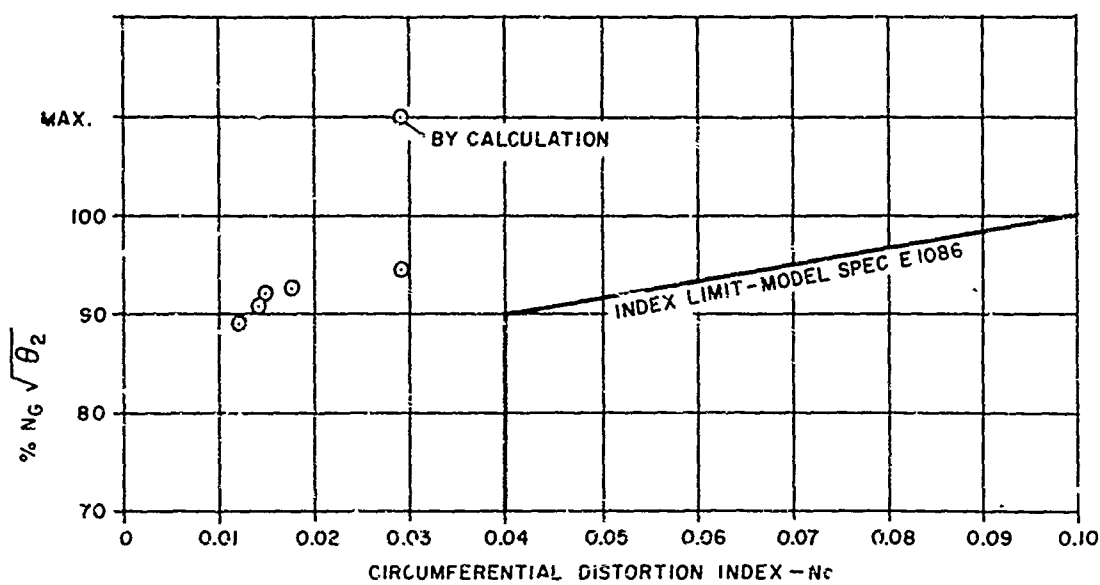


Figure 28. CV-7A/T64 Inlet Duct - Circumferential Distortion Average Across Annulus.

- θ_1^- = a single low-pressure area in the compressor annulus, measured in angular form, degrees.
- θ_1^+ = the largest high-pressure area adjacent to θ_1^- , degrees.
- θ_2^+ = the smallest high-pressure area adjacent to θ_1^+ , degrees.

The plotted points are arithmetical averages across the annulus of all six total pressure probes for separate airflow/RPM conditions. The one point at 100% $N_G / \sqrt{\theta_2}$ is derived from a ratio factor of PS_2 / PT_2 , which was thought to be representative of conditions at the higher flow.

Figures 29 through 33 show plots of ΔP for all six pressure probes at flow conditions of 7.97, 8.78, 9.30, 9.40, and 10.10 lb/sec. The plotted results at 0° and 180° suggest possible interference from the adjacent duct wall.

Figures 34 through 36 show plots of ΔP for the pressure probes at three flow conditions (8.11, 9.12, and 11.7 lb/sec), with the particle separator removed and replaced by a standard T58 bellmouth. With this configuration, it was found possible to achieve marginally higher flows; again, possible wall interference is noticeable at the 0° and 180° of rake travel. Probe number 6, at the greatest radius from the duct center line, indicates a greater ΔP than the remaining probes, especially in the vicinity of the duct wall over the lower 40° to 60°. At the 11.7 lb/sec condition, probe number 6 shows an increase in ΔP over a greater area than previously; this is probably the beginning of an increased distortion trend. This was the highest airflow achieved and is only 0.8 lb/sec below the required maximum for the system; therefore, distortion of a much greater magnitude is unlikely.

Figure 37, a plot of average radial distortion over 360° of annulus, shows the distinct region of distortion over the lower portion of the duct.

For the three highest speed conditions, with the exception of 94.35% RPM, the radial distortion is shown to exceed the 4% limit by approximately 1%. In the region of 180° rake position, the possible influence of the duct wall is again exhibited.

Figure 38 indicates the amount of radial distortion at a condition of 92.5% RPM. It can be seen to exceed the limit for that particular speed range by approximately 1%; further, referring to Table VI, it is the highest radial distortion factor experienced for all conditions. It is suggested that the 4% radial distortion limit is somewhat conservative when applied to the current T64 engine family; in the event of a 5% factor being experienced, it is thought to be unlikely that operating problems will result.

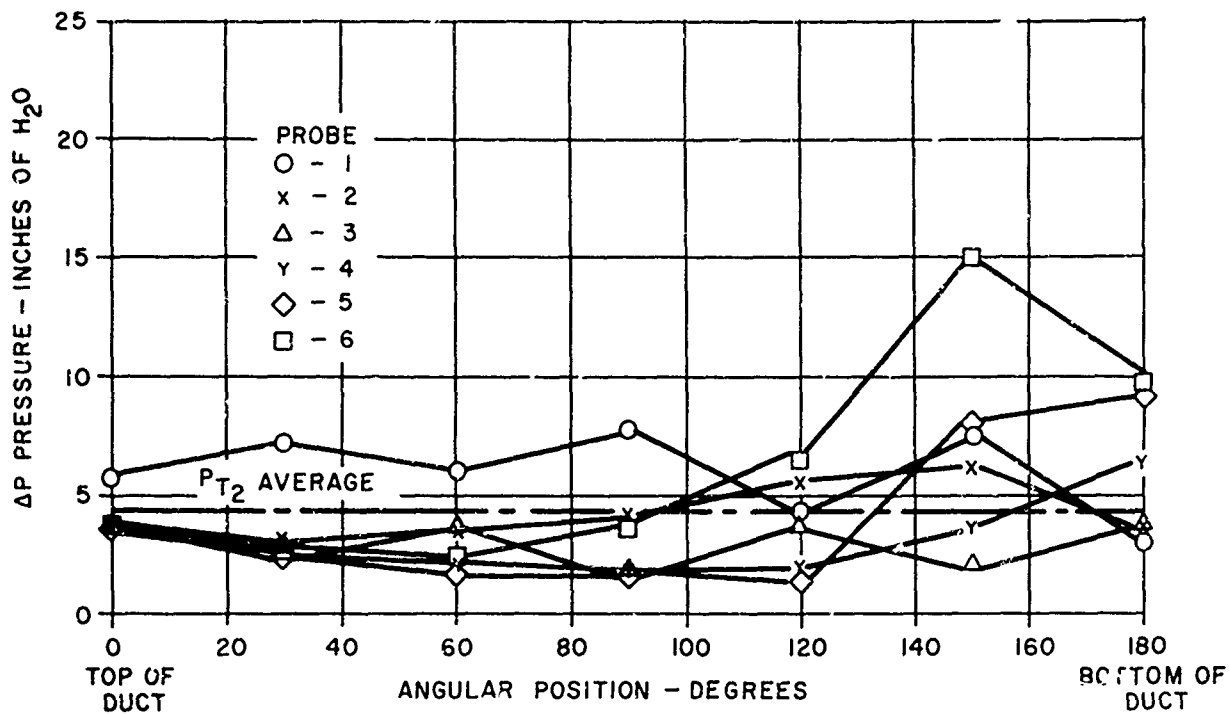


Figure 29. CV-7A/T64 Inlet Duct - Distortion Pattern at Flow of 7.97 Lb/Sec With Separator.

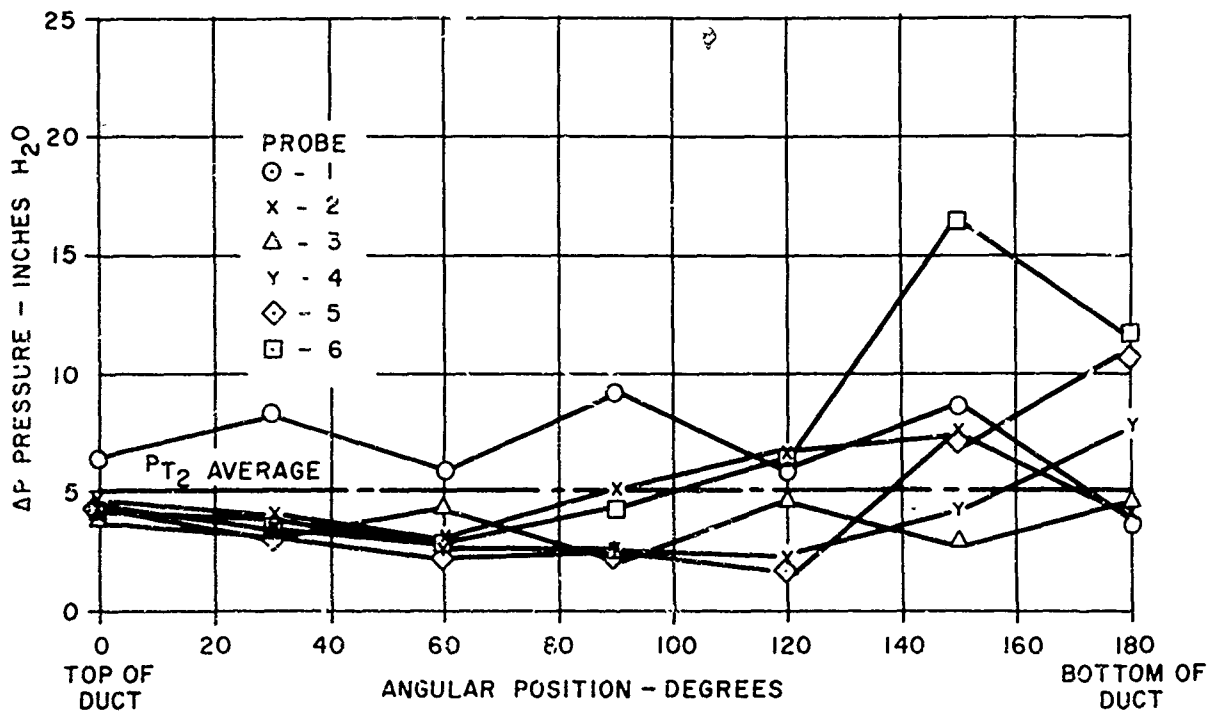


Figure 30. CV-7A/T64 Inlet Duct - Distortion Pattern at Flow of 8.78 Lb/Sec With Separator.

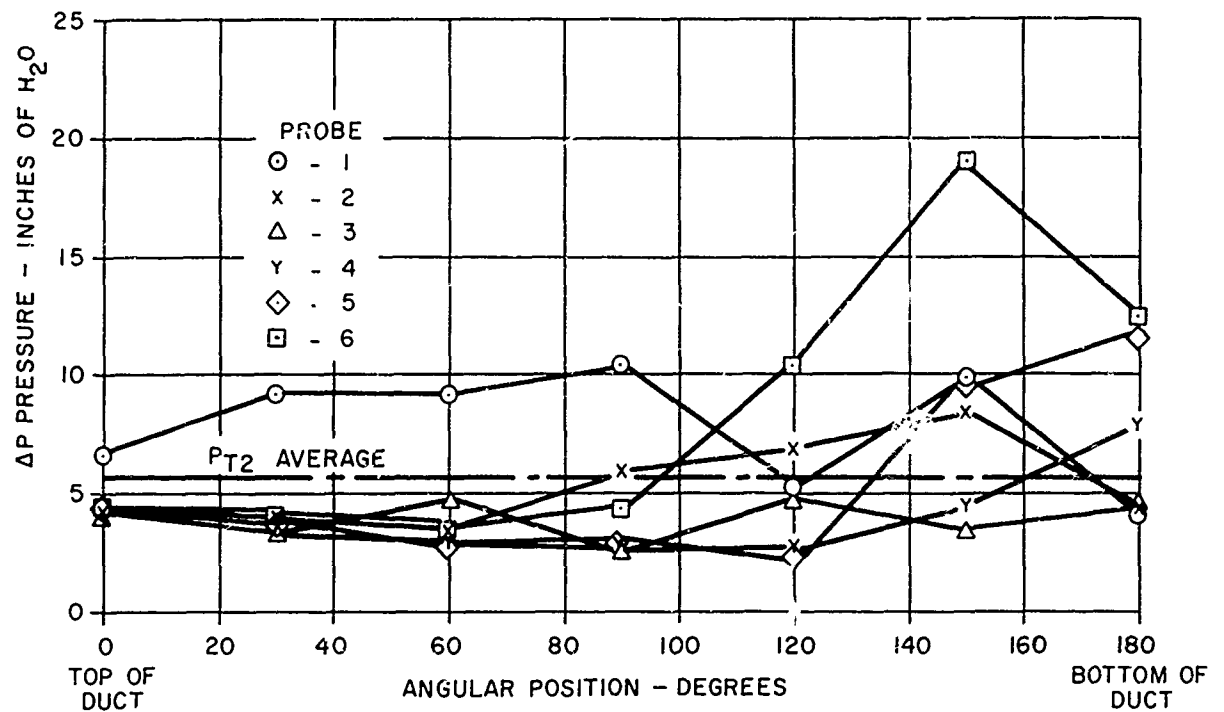


Figure 31. CV-7A/T64 Inlet Duct - Distortion Pattern at Flow of 9.3 Lb/Sec With Separator.

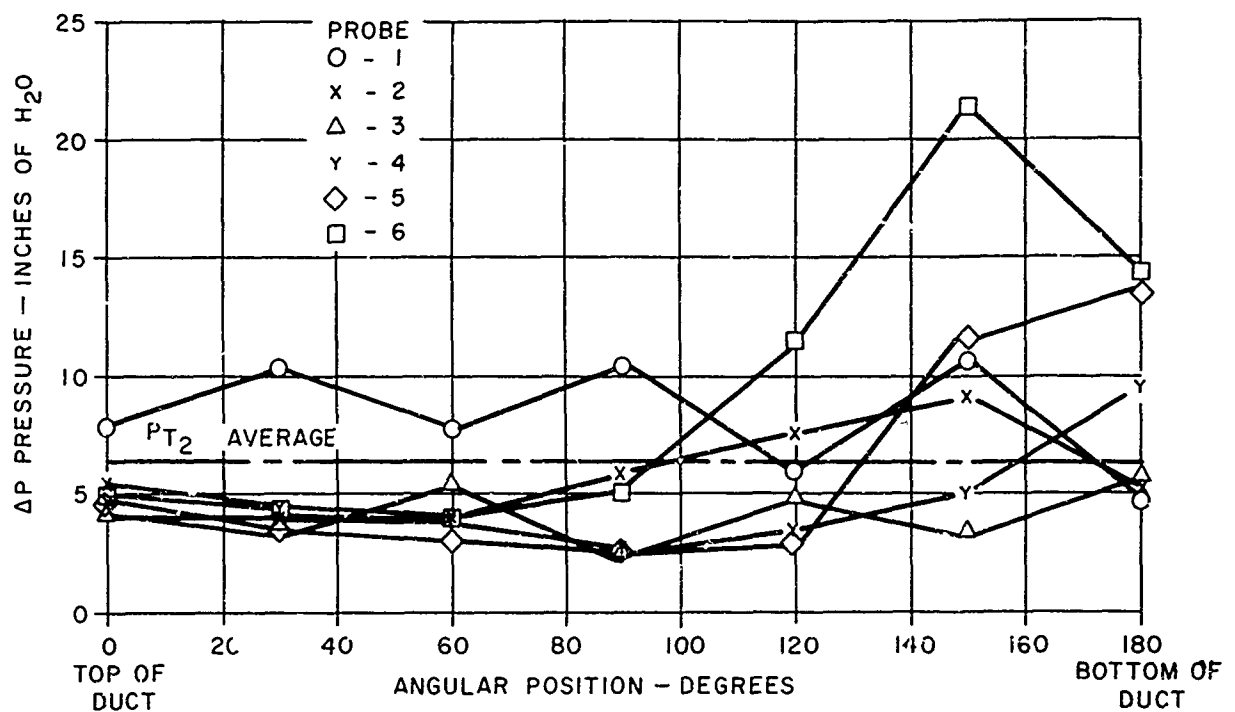


Figure 32. CV-7A/T64 Inlet Duct - Distortion Pattern at Flow of 9.4 Lb/sec With Separator.

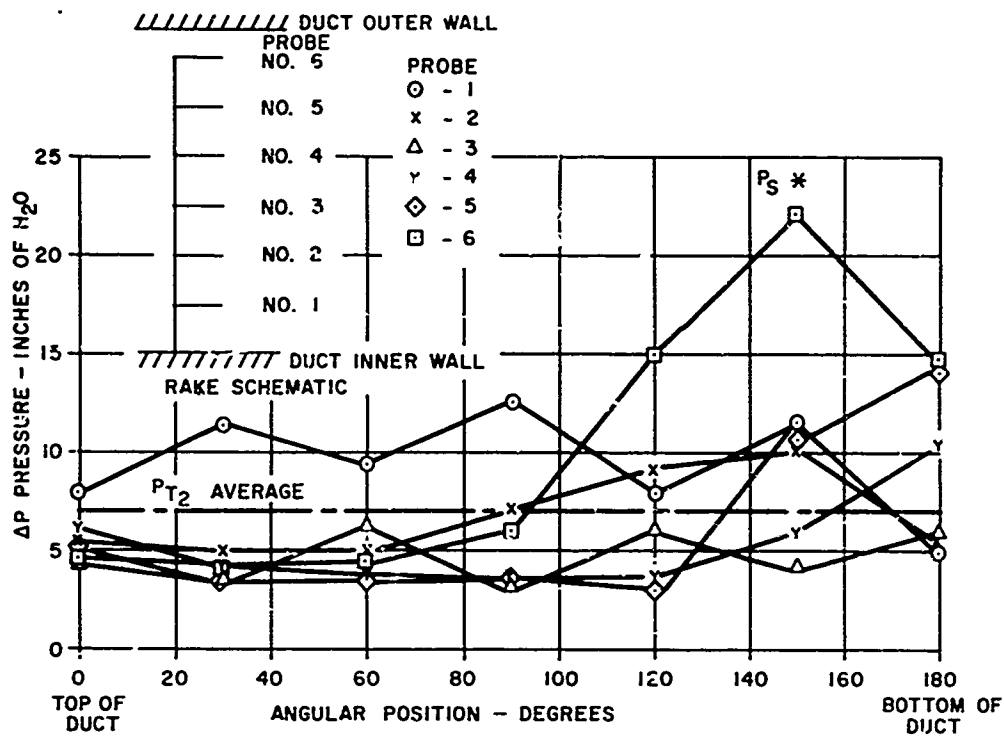


Figure 33. CV-7A/T64 Inlet Duct - Distortion Pattern at Flow of 10.1 Lb/Sec With Separator.

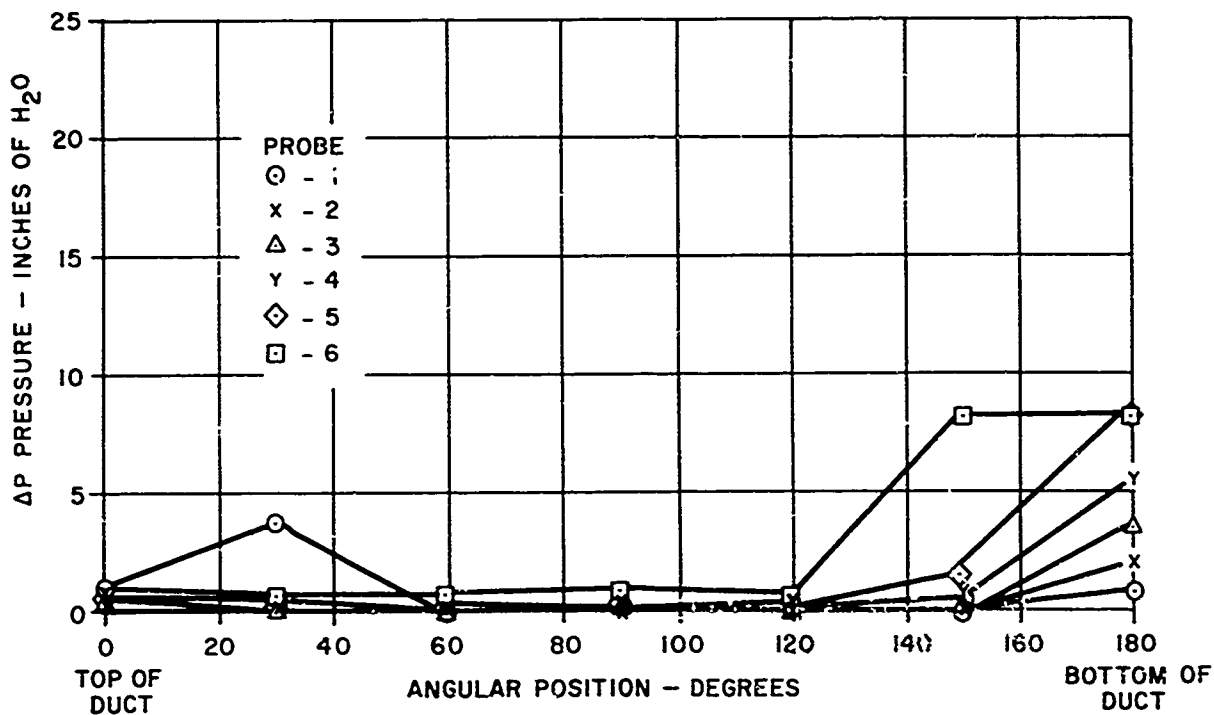


Figure 34. CV-7A/T64 Inlet Duct - Distortion Pattern at Flow of 8.11 Lb/Sec Without Separator.

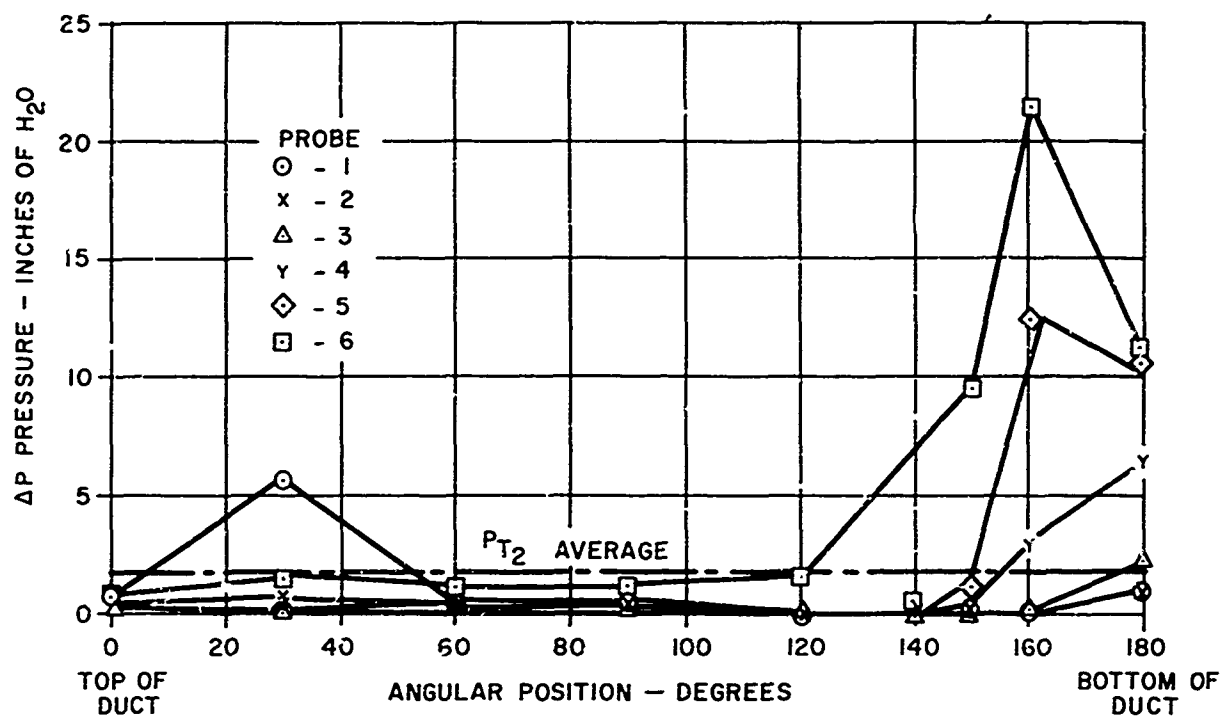


Figure 35. CV-7A/T64 Inlet Duct - Distortion Pattern at Flow of 9.12 Lb/Sec Without Separator.

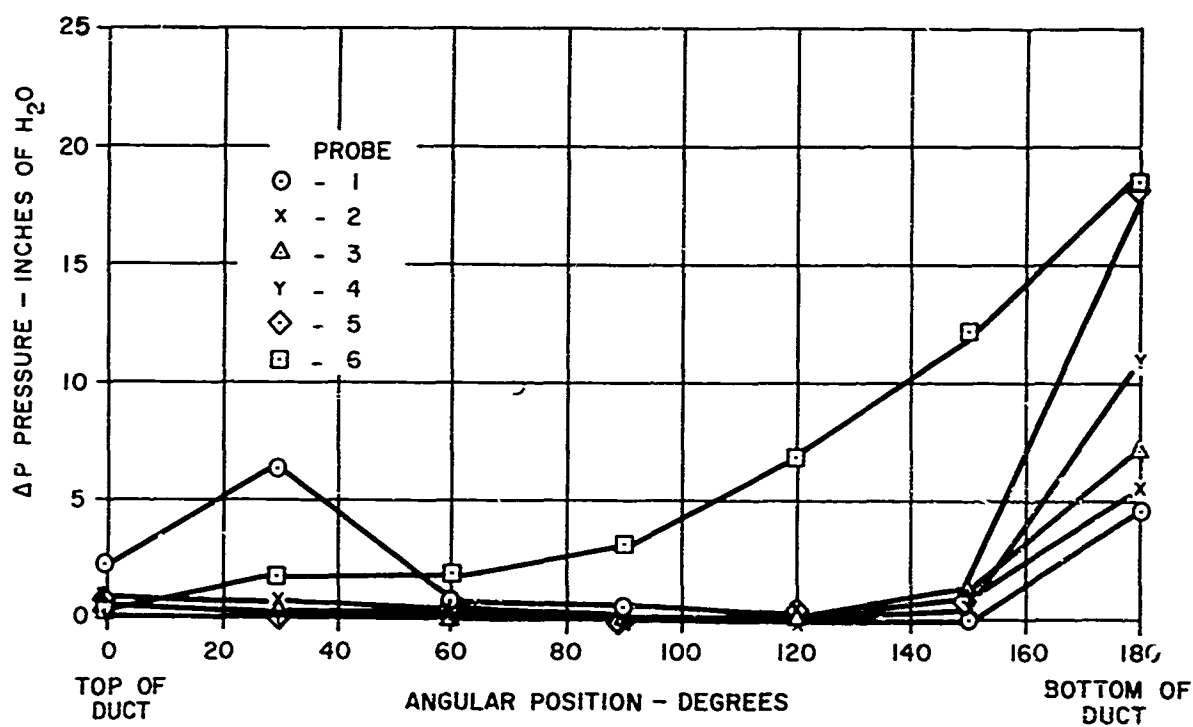


Figure 36. CV-7A/T64 Inlet Duct - Distortion Pattern at Flow of 11.7 Lb/Sec Without Separator.

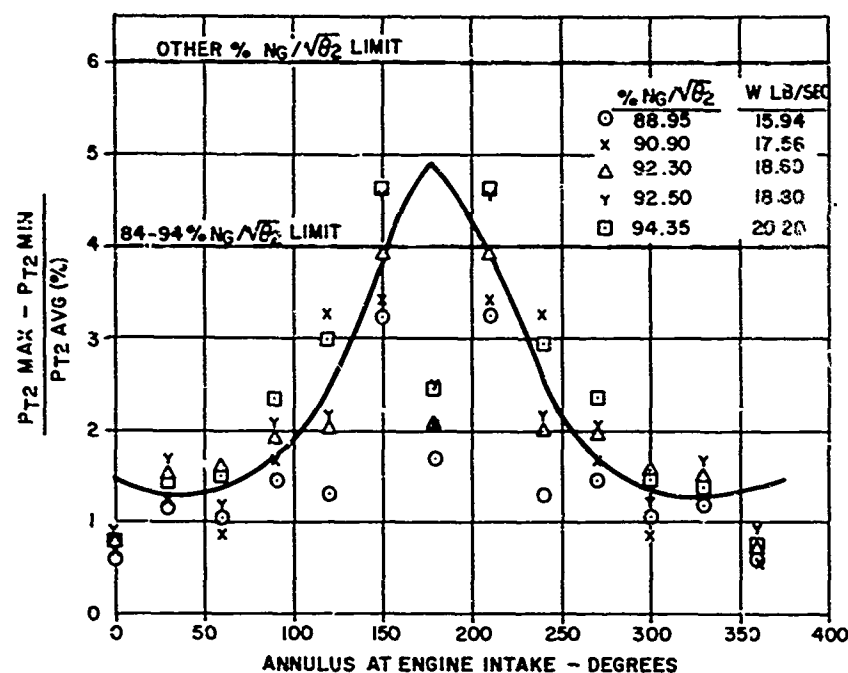


Figure 37. CV-7A/T64 Inlet Duct - Average Radial Distortion With Separator.

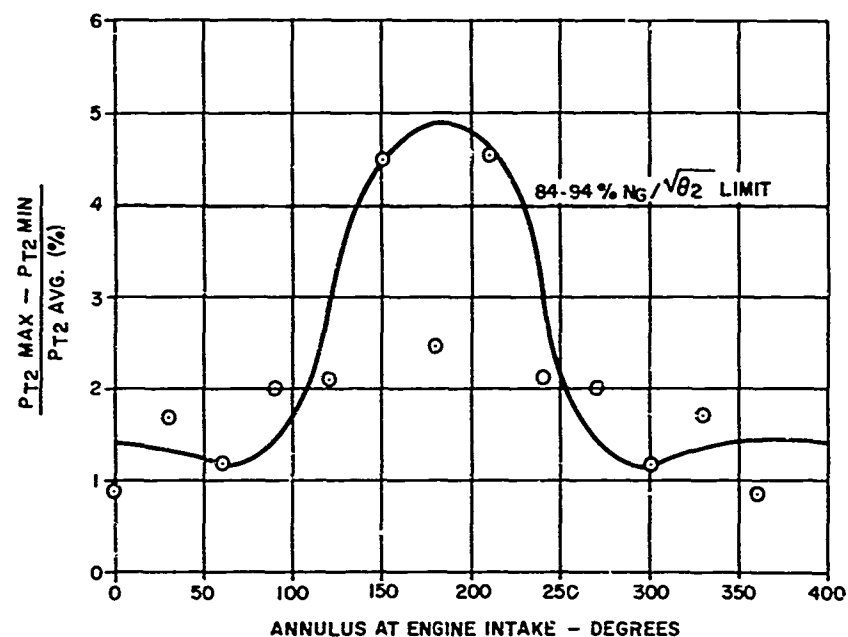


Figure 38. CV-7A/T64 Inlet Duct - Radial Distortion at 92.5% $N_G / \sqrt{\theta_2}$ With Separator.

Figure 39 is a plot of the arithmetic average radial distortion and the maximum recorded distortion which occurs at 150° . The average radial distortion for a given flow is derived from all probes at all annular positions. The distortion at 150° for a given flow is derived from all probes. The predicted results at the maximum flow condition of 25 lb/sec are shown, and it can be seen that the two limits of 4% and 6% for relative speed conditions are exceeded by .65% and .35% respectively.

Figures 40 and 41 indicate local static pressures along the length of the duct. The individual probe locations were measured from the separator exit and are duct wall distances.

Figure 40, which refers to conditions without the separator fitted, shows maximum local Mach numbers in the order of .460. This condition occurs at a point of rather severe flow turning; relating to the upswing of the curve, it suggests no evidence of flow breakaway.

Figure 41, which refers to a condition with a 1.6 lb/sec airflow reduction, and with the separator installed, shows maximum local Mach numbers in the order of .400. This condition also occurs at the most severe flow turn. The curves suggest no flow breakaway; rather, they show complete attachment.

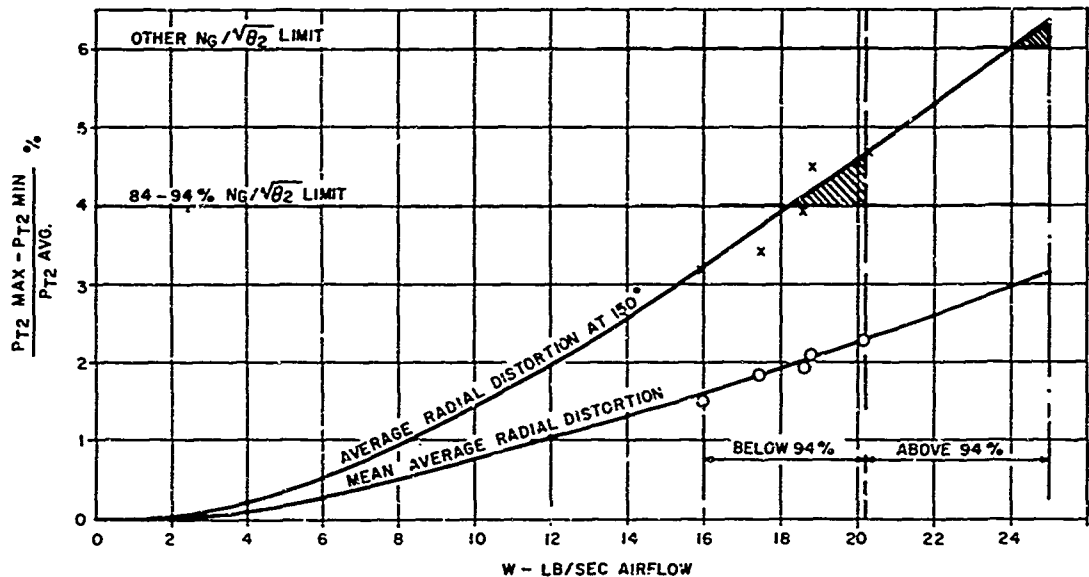


Figure 39. CV-7A/T64 Inlet Duct - Average and Maximum Angular Radial Distortion.

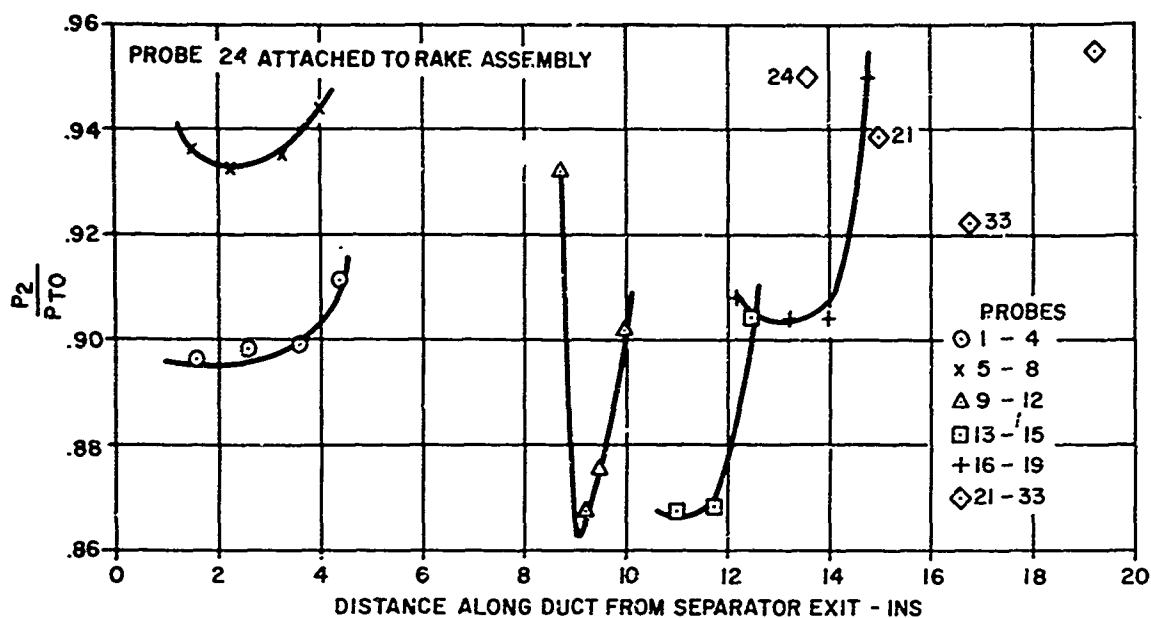


Figure 40. CV-7A/T64 Inlet Duct - Static Pressures Along Duct Flow - 11.7 Lb/Sec Without Separator.

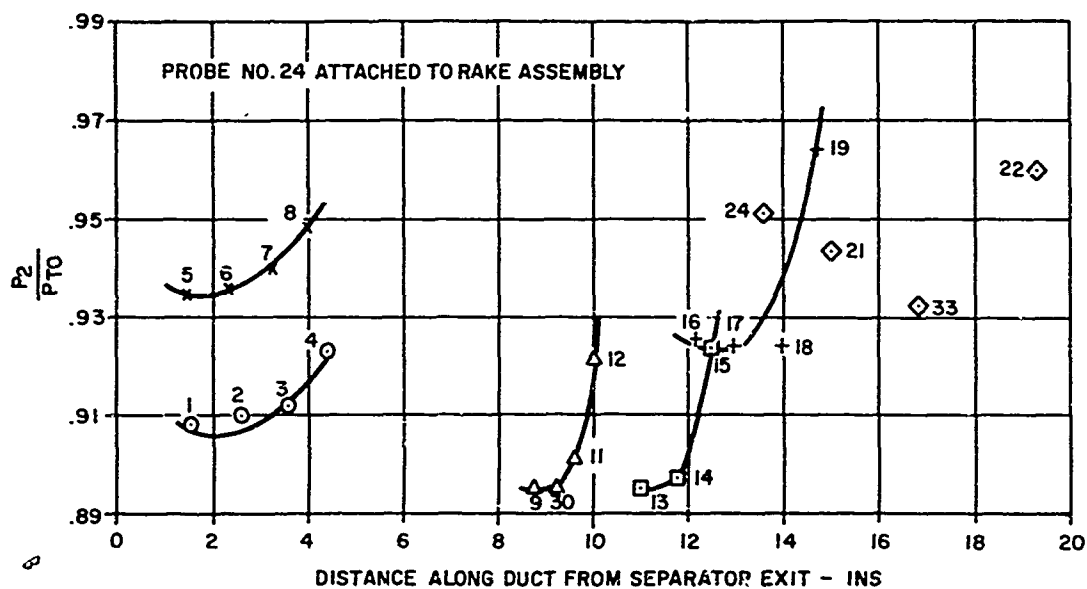


Figure 41. CV-7A/T64 Inlet Duct - Static Pressures Along Duct Flow - 10.1 Lb/Sec With Separator.

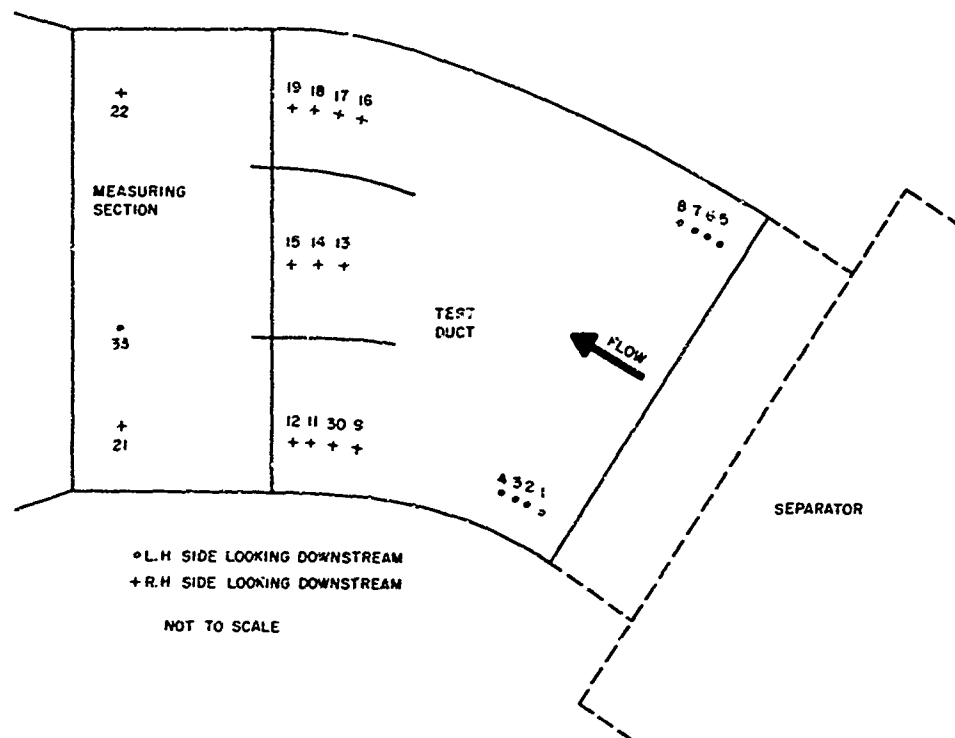


Figure 42. CV-7A/T64 Inlet Duct - Static Probe Locations.

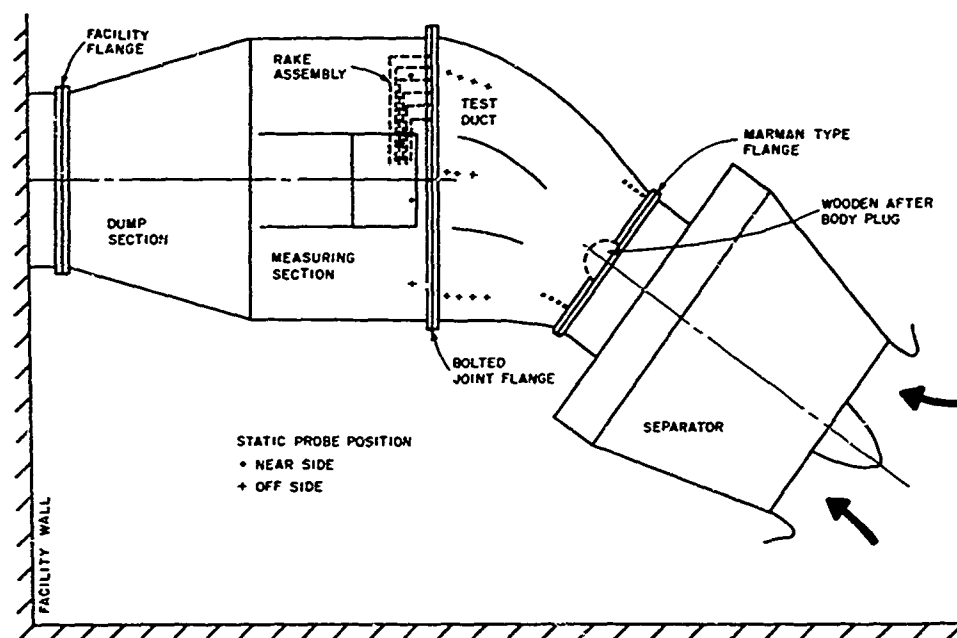


Figure 43. CV-7A/T64 Test Duct and Separator Layout.

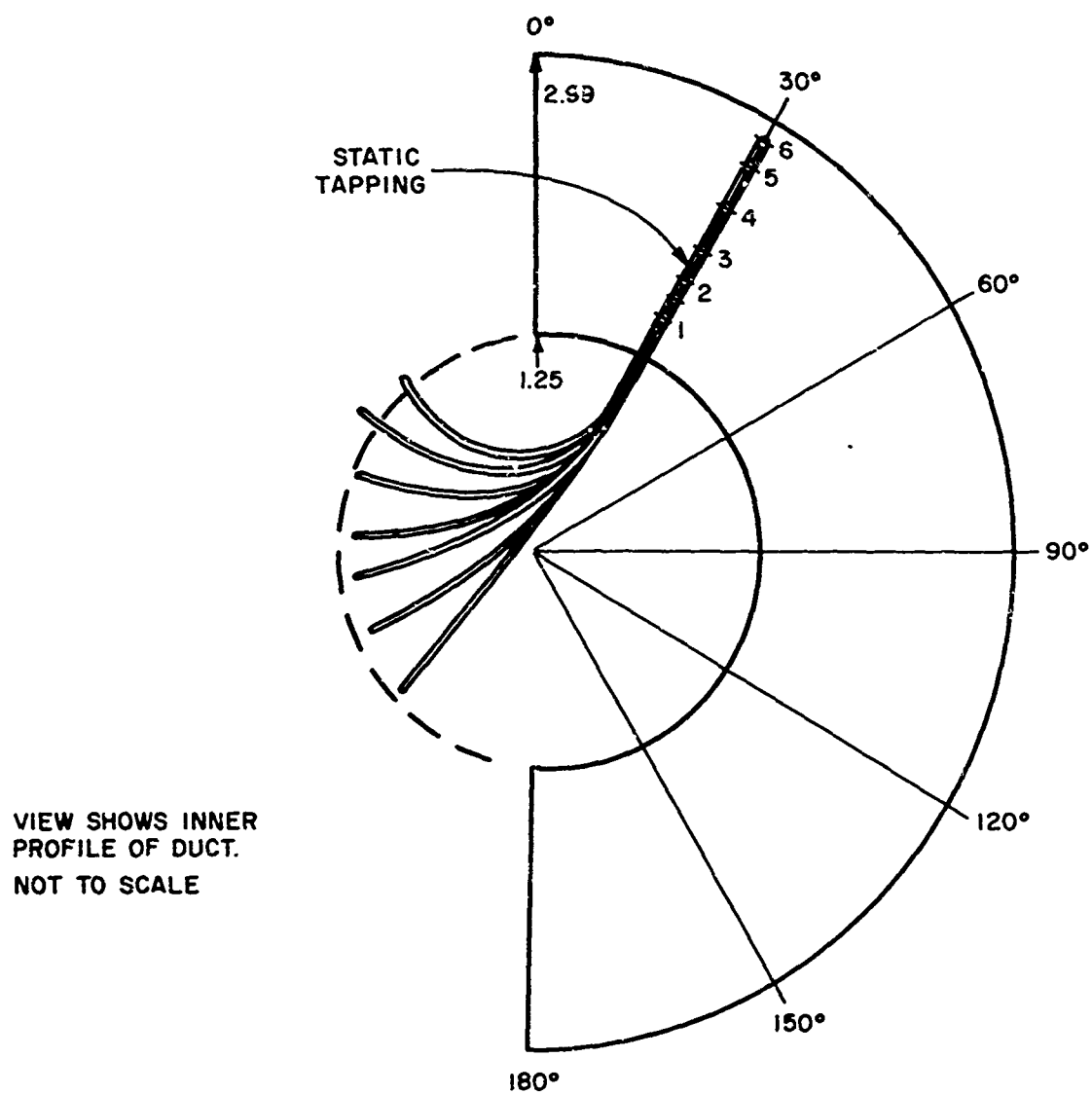


Figure 44. CV-7A/T64 Inlet Duct - Schematic of Test Duct Looking Downstream Showing Rake and Test Positions.

Probes 21, 22, 24, and 33 at flow conditions of 11.7 lb/sec without separator and 10.1 lb/sec with separator fitted indicate average Mach numbers of .295 and .281. Since these average values are derived from four static probe readings, three of which are marginally downstream of the measuring plans and the remaining one incorporated into the rake assembly, it is reasonable to expect the engine intake to be subjected to similar velocities.

The wooden afterbody plug fitted into the rear of the separator may possibly have influenced the test results because of its blunt, almost hemispherical profile. This was found to be necessary due to the configuration of the separator, which on a production type would permit the fitting of an optimum elliptical afterbody.

Table IV, from which Figure 37 is plotted, indicates the respective radial distortion factors at the various angular positions.

Table V reveals the relative capabilities of the various configurations.

As indicated, the programmed test duct is responsible for a 1.4% power loss and a .75% pressure recovery loss over and above the basic CV-7A duct configuration.

The particle separator contributes a further power loss of 2.45% and a pressure recovery loss of 1.35%, resulting in overall losses of 4.15% and 2.25% respectively.

The acceptability of the installed system will be dependent upon the margin of power loss that can be tolerated, without compromising the installation.

V. RESULTS

Results of the testing indicate the following trends and characteristics:

1. Distortion patterns at all flows tested exhibit a maximum distortion occurring in the lower 40° of the half annulus.
2. Probe results from the rake assembly indicate that the greatest severity of distortion occurs at probes 5 and 6; i. e., the two outer radii.
3. Distortion results at bottom dead center appear to be under considerable influence from the adjacent duct wall.
4. Radial distortion results show that the maximum values occur at 150° in the half annulus, and that at $92.5\% N_G / \sqrt{\theta_2}$, they exceed the 4% limit by approximately 1%.
5. Pressure recovery at the maximum flow condition of 12.5 lb/sec produces a loss of 2.25% (Table V).

VI. CONCLUSIONS

Based on the results of the test program, the following are concluded:

1. Pressure recovery at maximum airflow conditions of 25 lb/sec for the separator and downstream ducting is 97.75%.
2. The power loss at an airflow condition of 25 lb/sec is 4.15%.
3. Radial distortion is within limits in accordance with Spec. E. 1086 with the exception of the 92.5% $N_C / \sqrt{\theta_2}$ condition, where it is exceeded by approximately 1%.
4. Circumferential distortion index for all conditions is within limits in accordance with Spec. E. 1086.
5. The ducting, exclusive of the separator, contributes a pressure recovery loss of .75% and a power loss of 1.4%. This is not considered to be unreasonable for the configuration tested.
6. The duct exit distortion is of a 1/rev nature.
7. Relative to the foregoing conclusions, the duct and separator system is considered to be acceptable for installation.

VII. RECOMMENDATIONS

The following recommendations are made:

1. That flight testing be carried out at the earliest opportunity in order to substantiate model test data.
2. That all possible effort be made to increase the duct length between separator and engine, as is currently proposed by deHavilland, in order to minimize flow turning.
3. That ducting ahead of the separator be of an optimum design so as to reduce, as far as possible, any additional losses.

VIII. REFERENCES

1. Model Specification E1086, Engine, Aircraft, Turboprop. T64-GE-10 General Electric Company.

TABLE IV. RADIAL DISTORTION				
Flow Condition (lb/sec)	Rake Position	$\frac{P_{T2 \text{ Max}} - P_{T2 \text{ Min}}}{P_{T2 \text{ Ave}}} (\%)$	Limit (%)	$\%N_G / \sqrt{\theta_2}$
7.97	0	.59	4	88.95
	30	1.17		
	60	1.04		
	90	1.44		
	120	1.29		
	150	3.23		
	180	1.67		
8.78	0	.62	4	90.90
	30	1.27		
	60	.87		
	90	1.69		
	120	3.33		
	150	3.39		
	180	2.03		
9.30	0	.67	4	92.30
	30	1.50		
	60	1.59		
	90	1.94		
	120	2.00		
	150	3.92		
	180	2.06		
9.40	0	.87	4	92.50
	30	1.67		
	60	1.17		
	90	1.99		
	120	2.12		
	150	4.52		
	180	2.42		
10.10	0	.75	6	94.35
	30	1.45		
	60	1.50		
	90	2.35		
	120	2.98		
	150	4.62		
	180	2.47		

TABLE V. PRESSURE RECOVERY AND HORSEPOWER LOSS
AT 25 LB/SEC FLOW

Configuration	$\frac{P_{T2}}{P_{T0}}$	Compressor Face Total Pressure Inches of H ₂ O	Percent Shaft Horsepower Loss
Basic CV-7A Inlet Duct With and Without Prop.	.9985	405.4	.3
Test Duct Without Separator	.9910	402.3	1.7
Test Duct With Separator	.9775	397.	4.15
Relative to Basic CV-7A Duct, Test Duct contributes:			
1.7 - .3 = <u>1.4% ΔHP</u>			
3.1 "H ₂ O = .75% P_{T2}/P_{T0}			
Relative to Test Duct, Particle Separator contributes:			
4.15 - 1.7 = <u>2.45% HP</u>			
5.3 "H ₂ O = 1.35% P_{T2}/P_{T0}			

APPENDIX III
TEST RESULTS OF SEPARATOR DESIGN IMPROVEMENTS
ON FULL-SCALE FLOW MODEL

I. PURPOSE

To report the results of component testing of various separator modifications designed to improve separator performance.

II. DISCUSSION

1. Design Improvements

All separator design improvements were first tested in a full-scale model that was designed to allow testing of different separator configurations using the same basic model (Figure 45). For the tests described here, various combinations of six different separator parts were used in an effort to improve the separator performance. Figure 46 shows three different collection lip shapes, to scale, at their actual height above the separator hub radius and at their radial height in relation to each other. Figure 47 shows the two different hub hump contours that were used. The Number 1 hump contour (Figure 48) was sized to give constant axial annular area along the forward slope of the hump. For the Number 2 hump, the forward slope is the radial-plane profile of the steepest trajectory of a 25-micron particle as computed by trajectory analysis. The aft slope of both humps is just a smooth transition back to the original hub radius. A detailed analysis of the flow field, as was recommended, would aid in the design of these hub contours. A spacer that translates the inlet vanes axially forward 1.5 inches was also used for this test, but it is not shown in the figures.

The separator improvements described above were based on the fact that the separator efficiency is inversely proportional to the radius at which the particle is captured and the radius ratio of the separator. In fact, in a highly simplified solution of the particle trajectory equations (Reference 1), it is shown that the minimum particle size that a separator can collect is related to the above two parameters by

$$A_{\text{Min}} \propto R_2 \left(1 - \left(\frac{R_1}{R_2} \right)^4 \right)^{\frac{1}{2}}$$

where

A_{Min} = minimum particle diameter
 R_1 = separator hub radius at the beginning
of the swirl field
 R_2 = collection lip radius

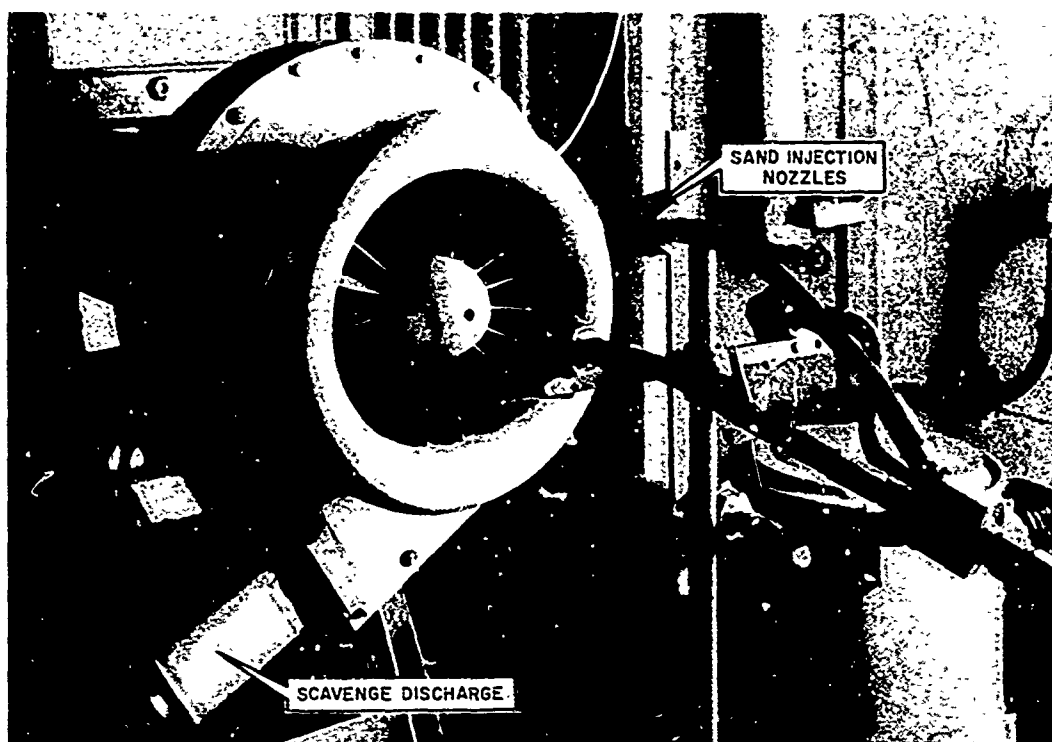


Figure 45. Full-Scale Flow Model on Component Test Stand.

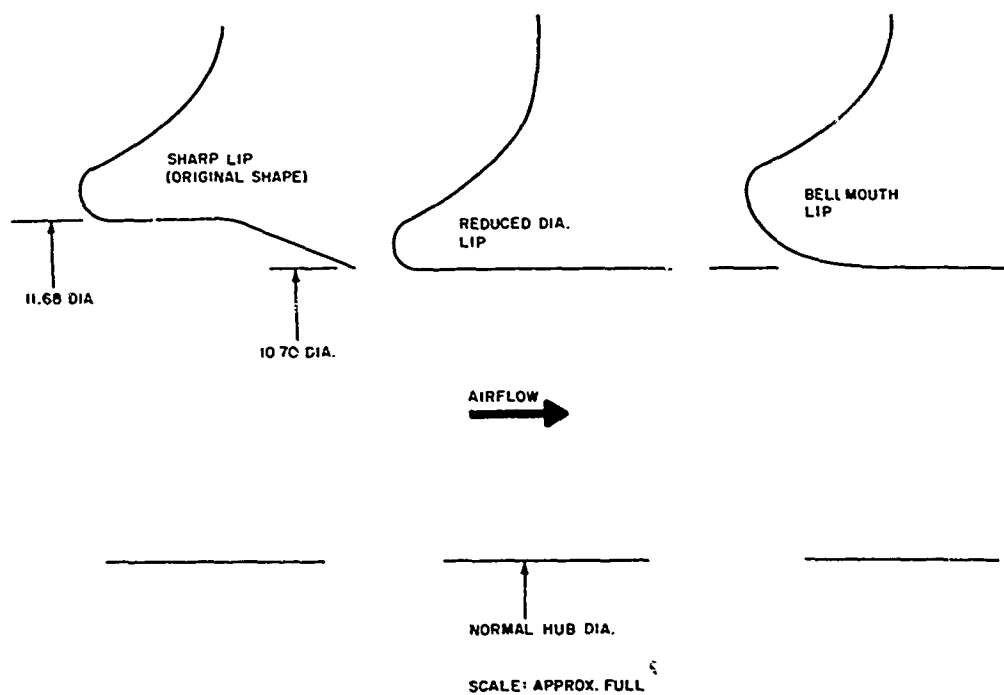


Figure 46. Comparison of Lip Shapes.

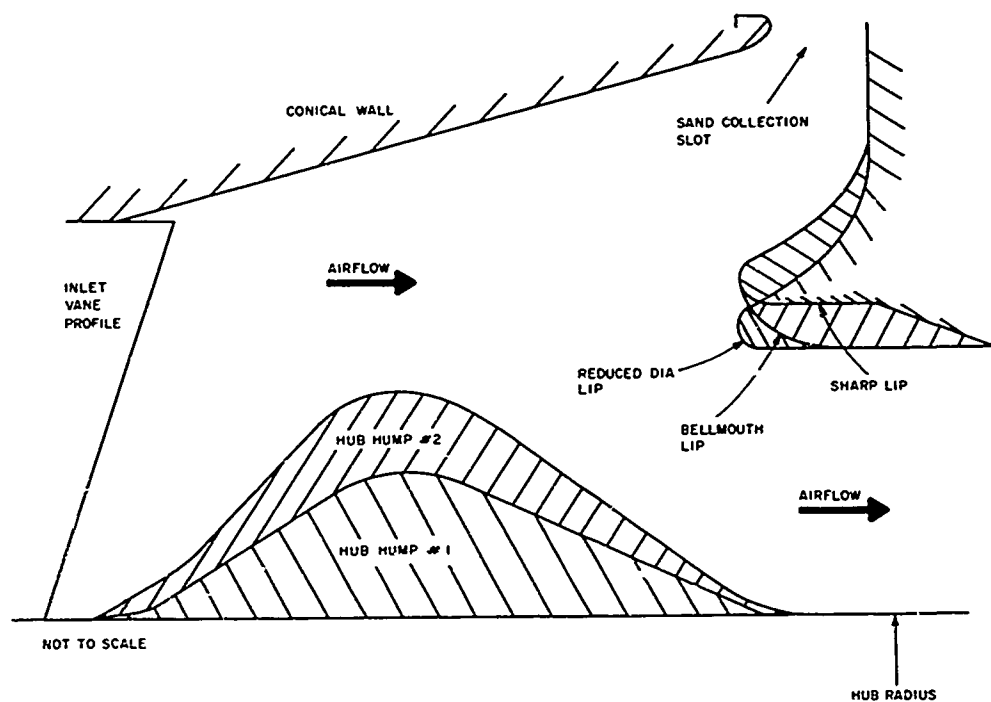


Figure 47. Schematic Cross Section of Separator Flow Model Showing Various Modifications.

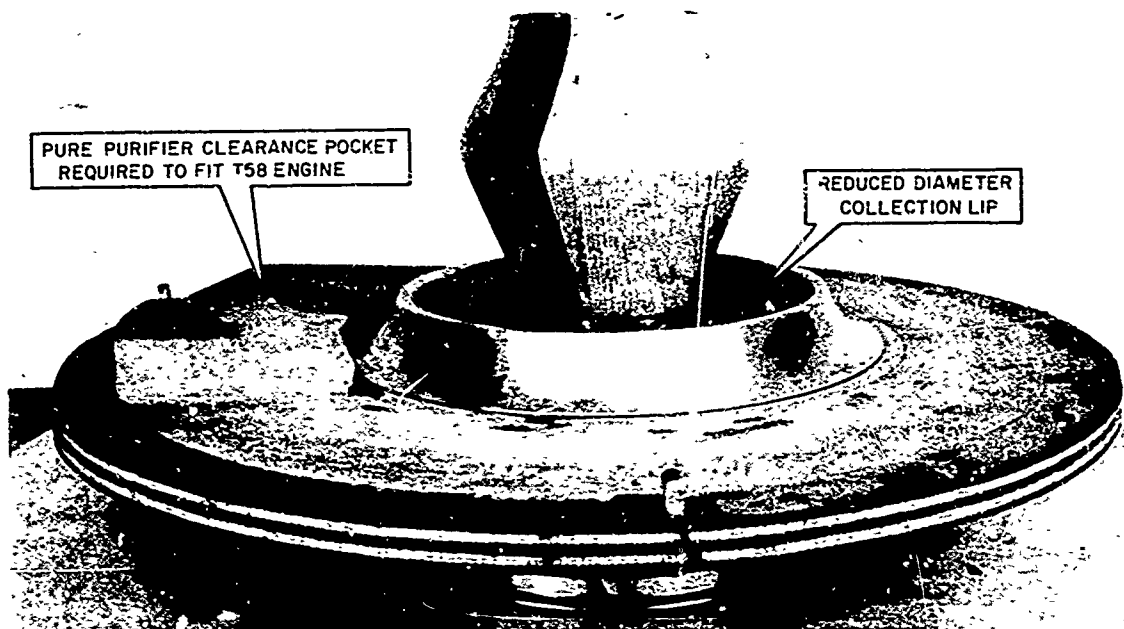


Figure 48. Number 1 Hub Hump on Separator Aft Wall.

As A_{min} decreases, collection efficiency increases.

Since it was easier to change the hub aft of the inlet vanes than to change the whole inlet vane cascade to increase R_1/R_2 , the hub humps were used. Also, putting the swirl in at a small hub radius gave the particles a larger initial acceleration due to the higher g -field. Reducing the collection lip radius, R_2 , gave the particle a shorter path to travel before it was collected, and it allowed the particle to be collected at a radius where the g -field was higher for a constant swirl angle.

To reduce the losses at the separator O. D., the inner contour of the collection lip was changed to an elliptical bellmouth shape. This change was not intended to increase collection efficiency.

2. Pressure Loss Measurement

Separator pressure loss was measured by the method described in Appendix I for those configurations which showed improvement in efficiency and for the 14" Standard.

3. Collection Efficiency Measurement

Efficiency on AC Coarse (ACC) test dust was used as the criterion for assessing collection efficiency improvement. ACC is a standard test dust of a controlled size distribution from 0 to 200 microns with a weight mean size of 30 microns. Since the present 738 Design separator (T58 Model) is 95% efficient with scavenge from 45 microns to 1500 microns, and since it is above 90% efficient without scavenge in the same particle size range, the collection improvement on particles smaller than 45 microns was of chief interest, and ACC is well suited to assess this improvement.

The glass beads used in some of the tests have a narrower size distribution than 0 to 200 microns, but their true size distribution is in doubt because of their very small absolute size. Microscopic analysis of the size AS and #380 beads gave weight mean particle sizes that were incompatible with the separator efficiencies on these beads. The beads have been shipped to the American Instrument Company, Silver Springs, Maryland, to be analyzed on their Aminco-Roller Analyzer, which is a standard device used in the metal powder industry for analyzing particles in the 0 to 800 microns range.

Collection efficiency for these tests is defined as the weight of the sand collected by the separator divided by the weight of the sand ingested.

4. Test Results

Table VI is a summary of all the tests conducted during this design improvement program. For those configurations where a qualitative assessment of pressure loss is given, pressure loss was not actually measured. The qualitative assessment is based on the facility blower damper setting required to pull the desired 12.5 lbs/sec through the separator. It was considered necessary to measure pressure loss for only those configurations which showed a sizeable collection efficiency increase or pressure loss reduction.

Figure 49 is a plot of the radial total pressure profiles aft of the separator for the four different configurations for which these data were taken. All the pressure loss numbers shown in Figure 47 were scaled to 12.5 lbs/sec separator main flow. Only an area weighted average of the pressure profiles was used to arrive at the total pressure loss. Most probably, a mass flow weighted average of the pressure profile would yield a lower total pressure loss.

The reduction in pressure loss at the separator O. D. due to the bellmouth lip is similar to that shown in Reference 1, but it is considerably greater. Reduction of the pressure loss at the I. D. due to the hub contouring was not an anticipated result, but it is not unreasonable. A detailed analysis of the 14" Standard flow field or a pressure survey would probably show that there is considerable separation from the hub. Installing the raised hub contour reduces the flow total velocity along the hub and shapes the flow path to reduce possible separation. This would reduce the hub losses and might even reduce an exit vane boundary layer separation problem along the lower 1/3 of the annulus height. Since the bellmouth lip helps at the O. D. and the hub hump helps at the I. D., it seems reasonable that combining these two changes would help, more than either alone, to reduce the separator pressure loss.

It can be seen from Table VI that the bellmouth lip seems to increase the collection efficiency by 2% on ACC. While this fact might be due to moving the lip stagnation point or to reducing the overall turbulence level in the separator, the true cause of the efficiency improvement is not known at this time. It would be more conservative to assume that the bellmouth lip reduces only the pressure loss and does not increase the collection efficiency.

Test numbers 21, 22, 24, 25, and 28 are 14" Standard configuration. The purpose of test number 28 was to make an assessment of stratification of the sand that passes the separator, by measuring the depth of erosion of a 1/4-inch diameter plastic rod inserted radially across the annulus, aft of the separator. Since the rod was at 1 o'clock position, the sand was fed in at 1 o'clock position

TABLE VI. TEST SUMMARY							
Radial Scroll Inlet Vanes @ 22° O.D. Stagger				Main Flow 12.5 PPS Corrected Scavenge Flow = 6% - 8%			
Test Date	Lip Shape	Hub Contour	Collection Length (Ins.)	Pressure Loss (Ins. H ₂ O)	Collection Efficiency On Size Shown	AC Coarse	
1	9/20/66	Bellmouth	Straight	7.6	5.25	-	-
2	9/21/66	Bellmouth	Straight	7.6	5.25	95%	-
3	9/21/66	Bellmouth	Straight	7.6	5.25	-	66%
4	9/21/66	Bellmouth	#1 3/16" AFT	7.6	5.25	-	66.4%
5	9/21/66	Bellmouth	#1 5/8" FWD	7.6	5.25	-	66%
6	9/21/66	Bellmouth	#1 17/32" AFT	7.6	5.25	-	66%
7	9/27/66	Reduced Dia	#1@Hub LE	7.6	Slight Increase	-	69%
8	9/27/66	Reduced Dia	#1@IGV TE	7.6	Slight Increase	-	67%
9	9/27/66	Reduced Dia	#1@IGV TE	9.1	Very High ΔPT	-	71%
10	9/27/66	Reduced Dia	#1@Hub LE	9.1	Very High ΔPT	-	72%
11	9/28/66	Reduced Dia	@ 1 7/8" AFT	9.1	Very High ΔPT	-	72%
12	9/28/66	Reduced Dia	#1@LE of Main Hub	9.1	Very High ΔPT	-	-
13	9/28/66	Reduced Dia	Straight	9.1	Slight In- crease over 6	-	73%
14	9/28/66	Reduced Dia	Straight	9.1	Slight In- crease over 6	-	71%
15	10/19/66	9899537-573	Flight Model	4.15"	H ₂ O ΔPT	-	-
16	10/19/66	Reduced Dia	Straight	7.6	7.06	-	70%
17	10/19/66	Reduced Dia	Straight	7.6	7.06	#380 96%	-
18	10/19/66	Reduced Dia	Straight	7.6	7.06	-	-
19	10/28/66	Reduced Dia	Straight	7.6	7.06	Size AS 33%	-
20	10/28/66	Reduced Dia	Straight	7.6	7.06	#380 96%	-
21	10/28/66	Sharp	Straight	7.6	6.87	-	63%
22	10/31/66	Sharp	Straight	7.6	6.87	-	-
23	10/31/66	Dyna clone efficiency check Nc = 100% on size AS beads					
24	10/31/66	Sharp	Straight	7.6	6.87	Size AS 41.6%	-
25	10/31/66	Sharp	Straight	7.6	6.87	#380 96%	-
26	11/ 3/66	Sharp	#2 1/4" AFT	7.6	7.12	-	71%
27	11/ 3/66	Sharp	#2 1/4" AFT	7.6	7.12	-	-
28	11/ 4/66	Sharp	Straight	7.6	6.87	-	66%
29	11/ 7/66	Sharp	#2 1/4" AFT	7.6	7.12	#480 97%	-
30	11/ 7/66	Sharp	#2 1/4" AFT	7.6	7.12	Same as 40%	-
31	11/ 7/66	Sharp	#2 1/4" AFT	7.6	-	-	No Scav. 47%
* Dimension is distance from hub L.E. to L.E. of Hub Hump.							

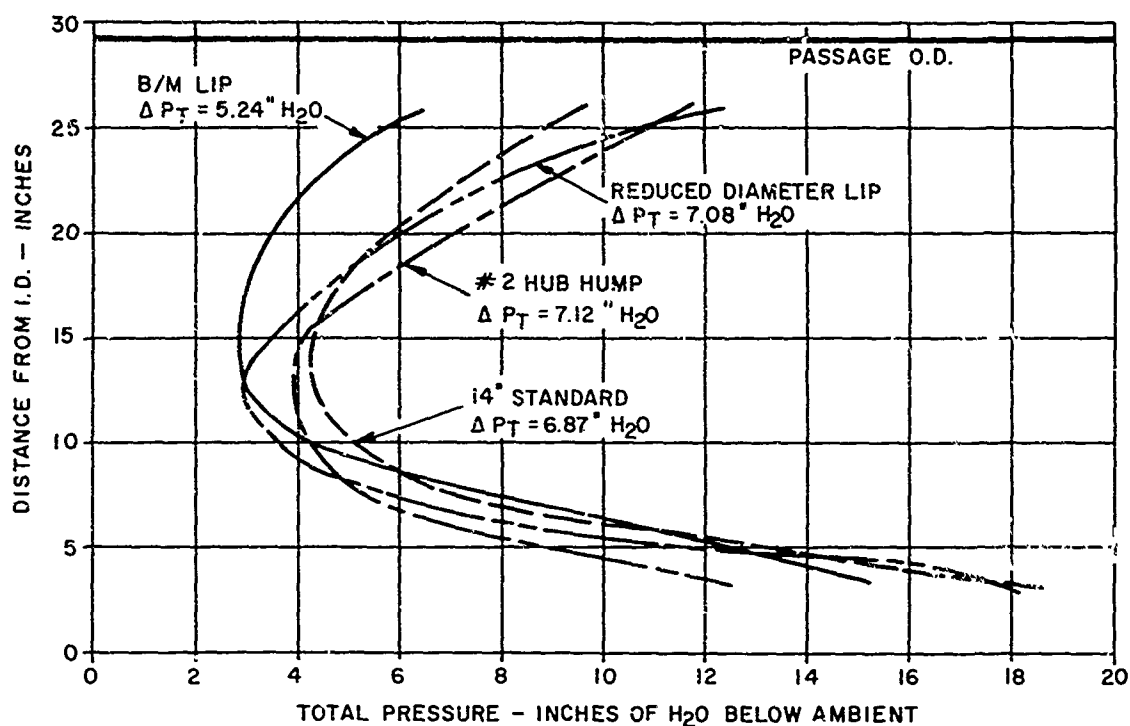


Figure 49. Total Pressure Profiles Aft of Separator.

to get maximum rod erosion; this might explain the high ACC efficiency compared to test number 21. The rod erosion was insufficient to be conclusive, and this phase of the testing was eliminated until the flight type T58 model is available and a coarser sand can be used. Coarse sand is not used with the wood flow model because the exit vanes are a hard plastic and are subject to erosion.

Since a flight type sheet metal configuration of a separator with a hub contour has not been built, the true improvement offered by hub contouring in a flight type separator can only be assumed based on experience. The T58 separator efficiency on ACC is 68%, which is 4 to 5% higher than the wood model on which the T58 model was based. This efficiency increase was probably due to the aerodynamically cleaner flow path of the T58 model compared to the flow model. For this reason, it is assumed that a T58 model with the number 2 hub contour would be 75 to 76% efficient on ACC. Pressure loss for this modified T58 model would probably increase .05% to 1.4% - an amount similar to that seen on these model tests for the addition of the hub contour. It should be noted that the repeatability of the pressure loss measurement is no more than ± 0.4 inch H₂O (.1% P_{T0}).

There is almost as much payoff in efficiency increase from the reduced diameter lip as from the hub hump. With the axial spacer, the reduced diameter lip configuration is more efficient than the hub hump configuration. The spacer would make the separator longer, which is undesirable, and the reduced diameter lip would probably be incompatible with the number 2 hub hump. For this reason, the bellmouth lip with the number 2 hub contour (Figure 6) was chosen as the most promising in terms of increasing collection efficiency and reducing pressure loss. Of course, the reduced diameter lip would not be ruled out without further testing or analysis.

III. CONCLUSIONS

1. The configurations tested compare as listed below:

<u>Configuration</u>	<u>Pressure Loss</u>	<u>Collection Efficiency on AC Coarse Test Dust</u>
A. 14" Standard	1.69%	64%
B. Bellmouth Lip	1.29%	66%
C. Reduced Diameter Lip	1.74%	70%
D. 1/4" Standard Plus number 2 Hub Contour	1.75%	71%

2. If the same performance increase were made in going from a wood model of configuration D, above, to a flight-type model of configuration D, as was made in going from configuration A to the T58 separator 9899537-738, then the performance of the flight-type model of configuration D would be:

Pressure loss at 10,000 CFM	1.4%
Collection efficiency on AC Coarse with scavenge	75%
Weight of 10,000 CFM separator exclusive of scavenge system	19 lbs
Length of separator (flange to flange)	14 in

IV. RECOMMENDATIONS

1. Test a separator having the number 2 hub contour plus the bellmouth lip (see Figure 50). Based on testing to date, this configuration will probably reduce separator pressure loss and increase the collection efficiency.

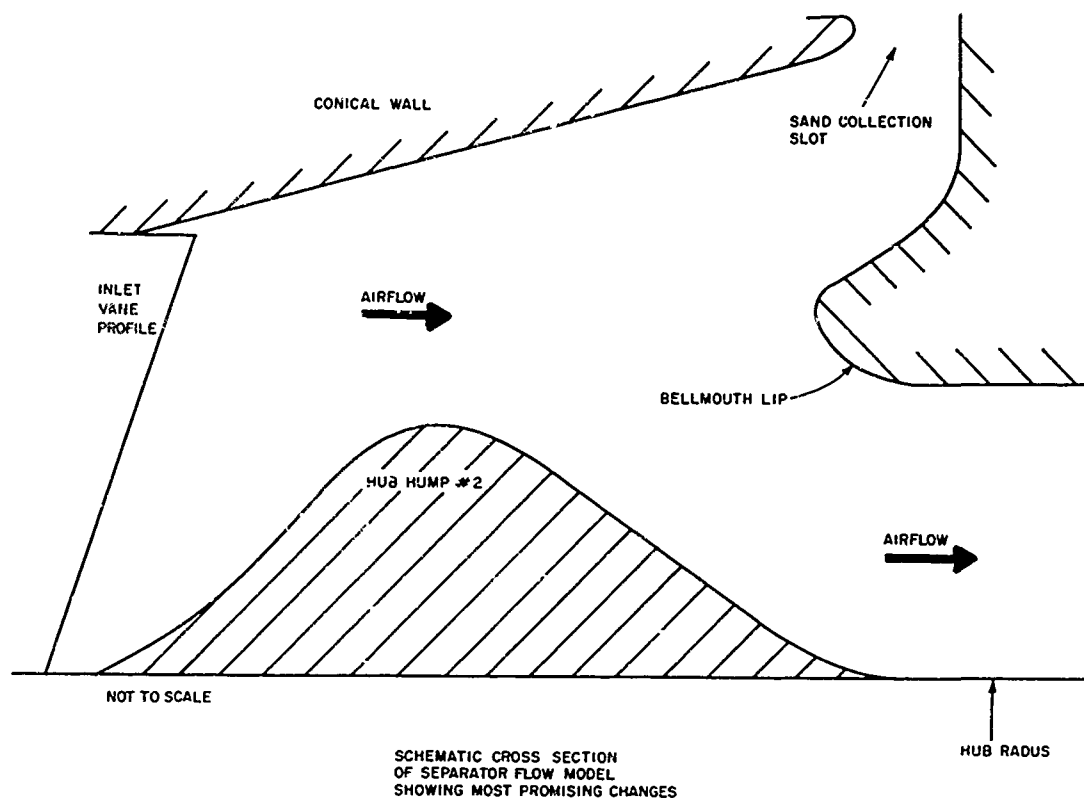


Figure 50. Schematic Cross-Section of Separator Flow Model Showing Most Promising Changes.

2. Test other possible separator improvements such as:

- 18° cone angle barrel
- larger hub hump contour
- bellmouth lip plus higher inlet vane stagger
- conical wall vortex generators to reduce wall separation and to extend the swirl field closer to the collection slot.
- reduced scavenge scroll flow area.

Each of these changes was suggested because of previous test experience with the separator.

3. Make an analysis of the separator flow field using the Compressor Axisymmetric Flow Distribution program. This analysis would be used to change the separator contour to further increase collection efficiency and to decrease pressure loss. A similar analysis was used during the design of the 738 Design separator and was of great benefit to the success of that design.

Defense Documentation Center
First Cavalry Division (Airmobile)

20

1

2

Unclassified

Security Classification

DOCUMENT CONTROL DATA - R & D		
(Security classification of title, body of abstract and indexing annotation must be entered when the overall report is classified)		
1. ORIGINATING ACTIVITY (Corporate author) General Electric Company West Lynn, Massachusetts		2a. REPORT SECURITY CLASSIFICATION Unclassified
		2b. GROUP
3. REPORT TITLE DESIGN AND COMPONENT TEST ON ENGINE AIR INLET PARTICLE SEPARATOR FOR THE CV-7A AIRCRAFT		
4. DESCRIPTIVE NOTES (Type of report and inclusive dates) Final Technical Report		
5. AUTHOR(S) (First name, middle initial, last name) R. J. Duffy		
6. REPORT DATE August 1968	7a. TOTAL NO. OF PAGES 79	7b. NO. OF REFS 5
8a. CONTRACT OR GRANT NO. DA 44-177-AMC-343 (T)	8b. ORIGINATOR'S REPORT NUMBER(S) USAAVLABS Technical Report 68-48	
9. PROJECT NO. 1T062103A047		
c. 4.	9b. OTHER REPORT NO(S) (Any other numbers that may be assigned this report) TM68AEG1441	
10. DISTRIBUTION STATEMENT This document has been approved for public release and sale; its distribution is unlimited.		
11. SUPPLEMENTARY NOTES	12. SPONSORING MILITARY ACTIVITY US Army Aviation Materiel Laboratories Fort Eustis, Virginia	
13. ABSTRACT An inlet protection system for the CV-7A aircraft's T64-GE-8 engine is described in this report. Separator design, special manufacturing problems, and component test results are presented and discussed. Additional background information describing previous work from which the CV-7A separator design evolved is included where applicable. Component efficiency tests indicate that separator collection efficiencies exceed contract requirements. Pressure loss measurements, taken coincident with the efficiency test, indicate a pressure drop greater than design limits. Engine testing, not included in the modified contract work scope, would be required to accurately define the result of increased pressure loss on installed engine performance.		

DD FORM 1473

REPLACES DD FORM 1473, 1 JAN 64, WHICH IS OBSOLETE FOR ARMY USE.

Unclassified

Security Classification

Unclassified

Security Classification

14.	KEY WORDS	LINK A		LINK B		LINK C	
		ROLE	WT	ROLE	WT	ROLE	WT
	Turboprop/Turboshaft Engine Air Inlet Particle Separator Inlet Protection System for CV-7A Aircraft T64-GE-8 Engines Bench Testing Engine Air Inlet Particle Separators Air Cleaner Design with a High Flow per Unit Area Separator Weight Separator Installation Facility Calibration Separator Pressure Loss Measurement Separator Collection Efficiency Measurement Testing with Coarse and Fine Sand						

Unclassified

Security Classification

9118-68